

Funded by the  
European Union



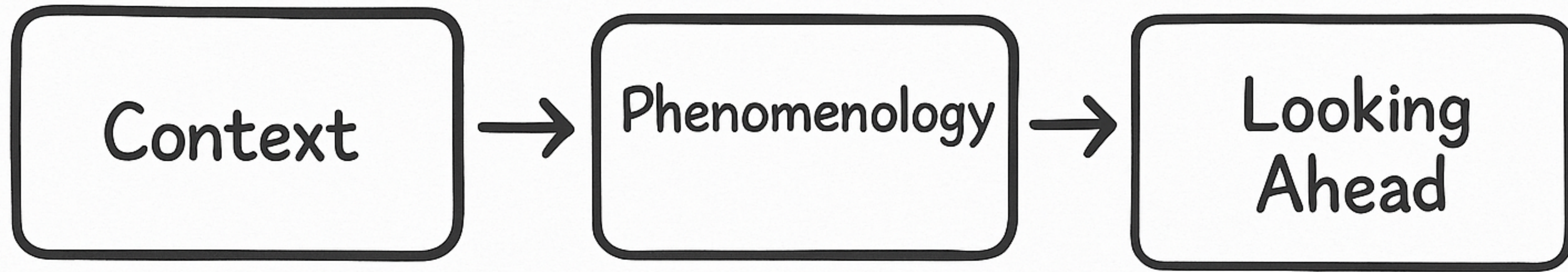
# Probing ultralight axion-like particles with quantum technology

Sreemanti Chakraborti





# Plan of the Talk

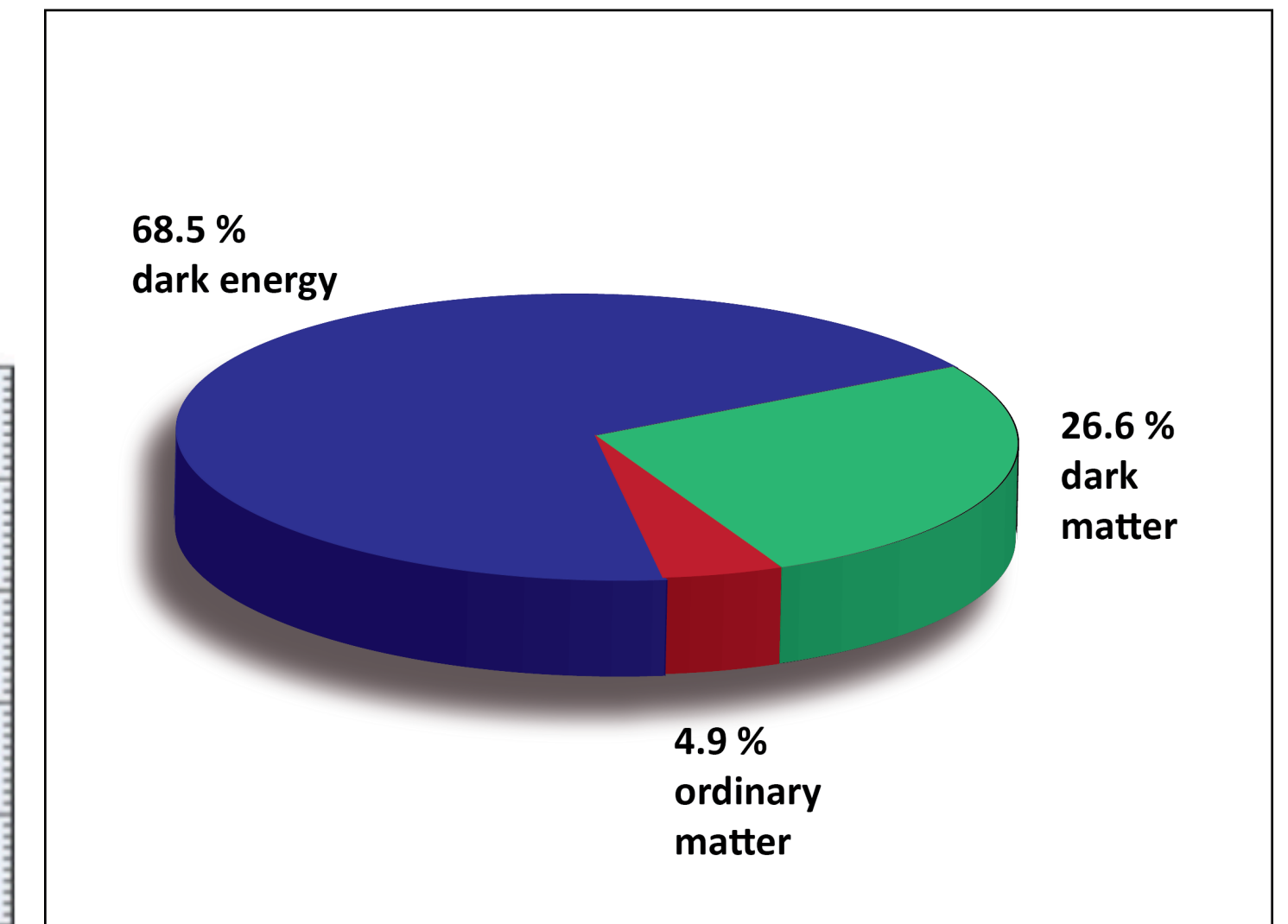
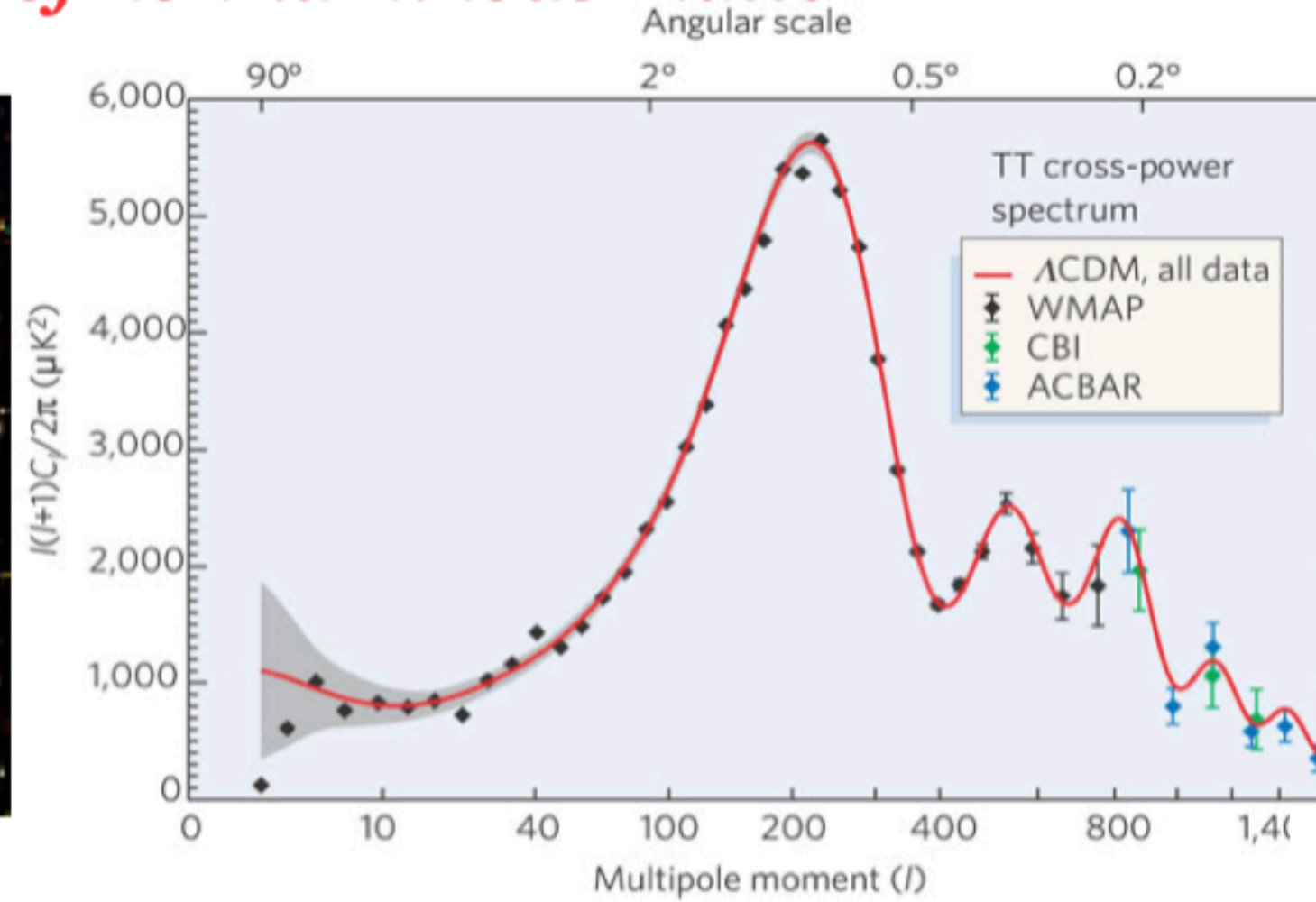
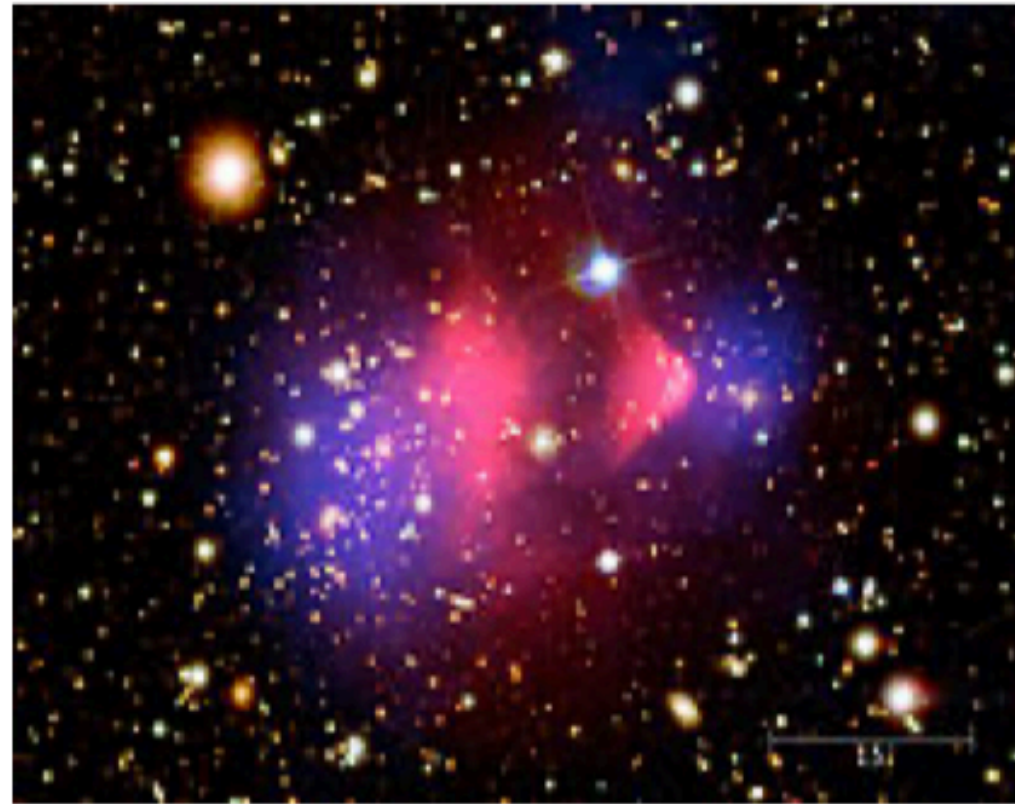
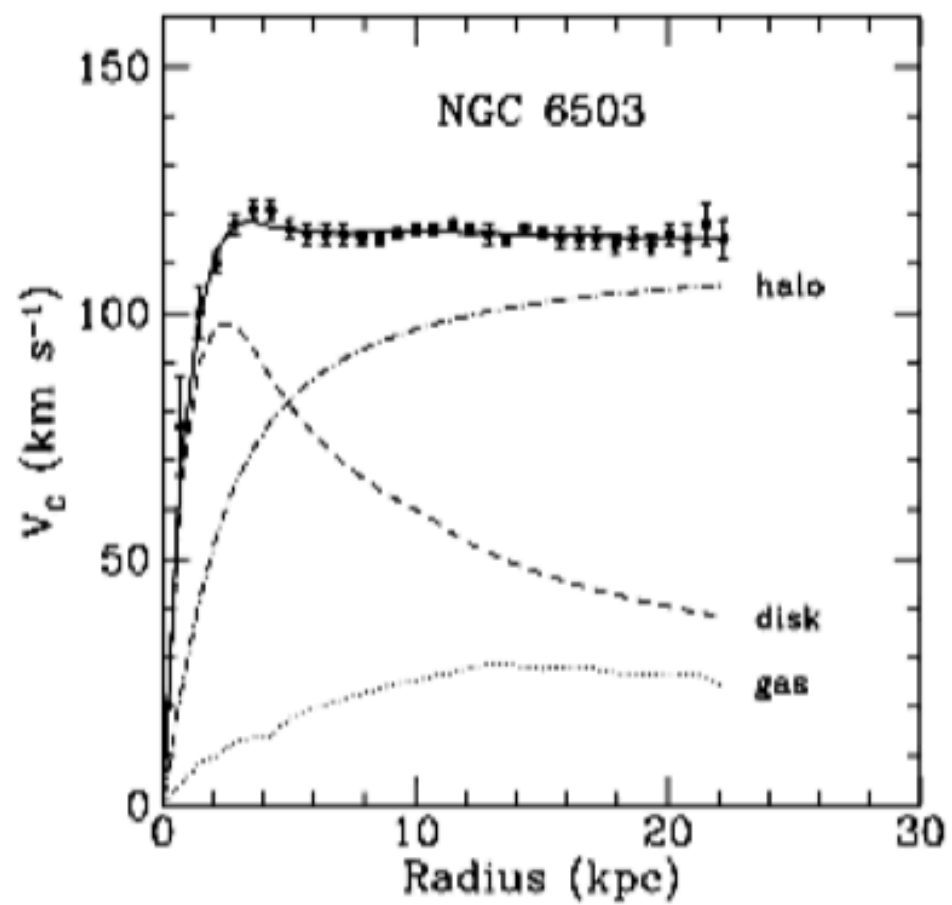




# Context

# Dark matter

*Compelling evidence (only gravitational) of non-luminous matter*



***We know...***

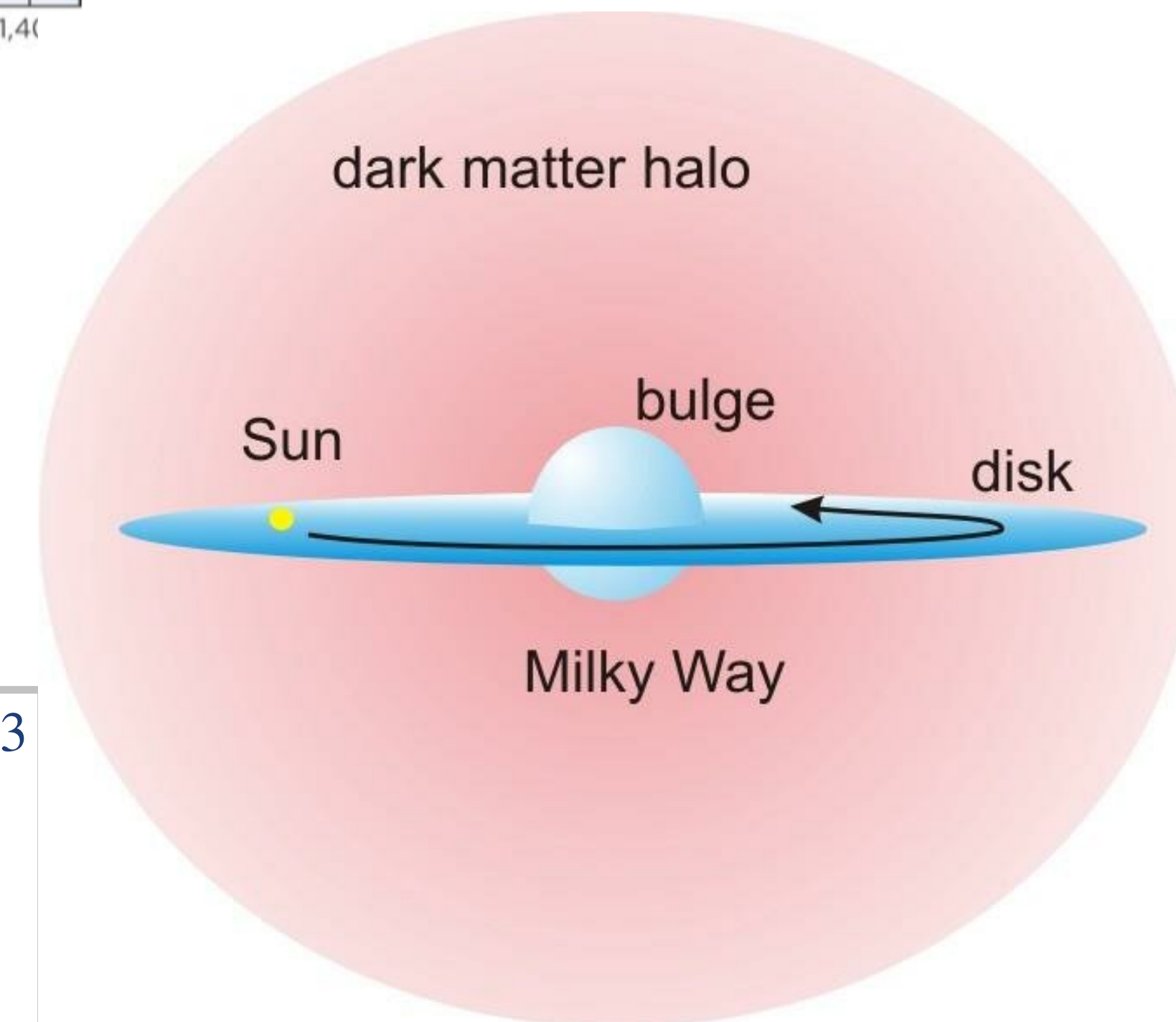
- its abundance
- pressureless
- long-lived enough
- neutral enough

***We don't know...***

- fundamental particle?
- spin, mass?
- non-gravitational interactions?
- **thermal relic?**
- when was it produced?
- ...

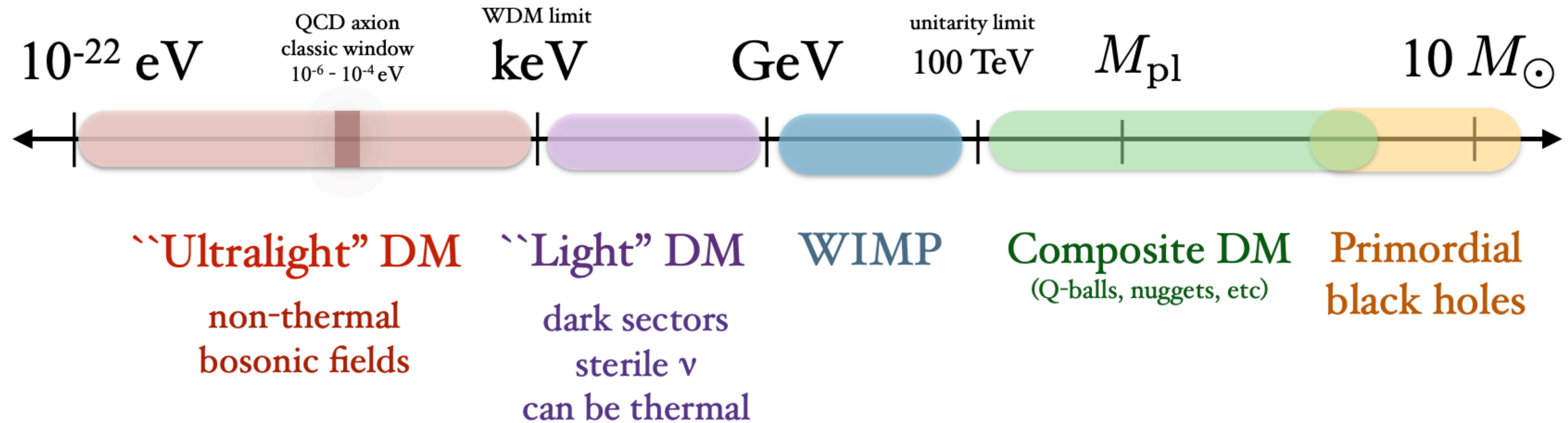
$$\rho_{\text{DM}}^{\text{local}} \approx 0.4 \text{ GeV/cm}^3$$

$$v_{\text{DM}} \sim 300 \text{ km/s}$$





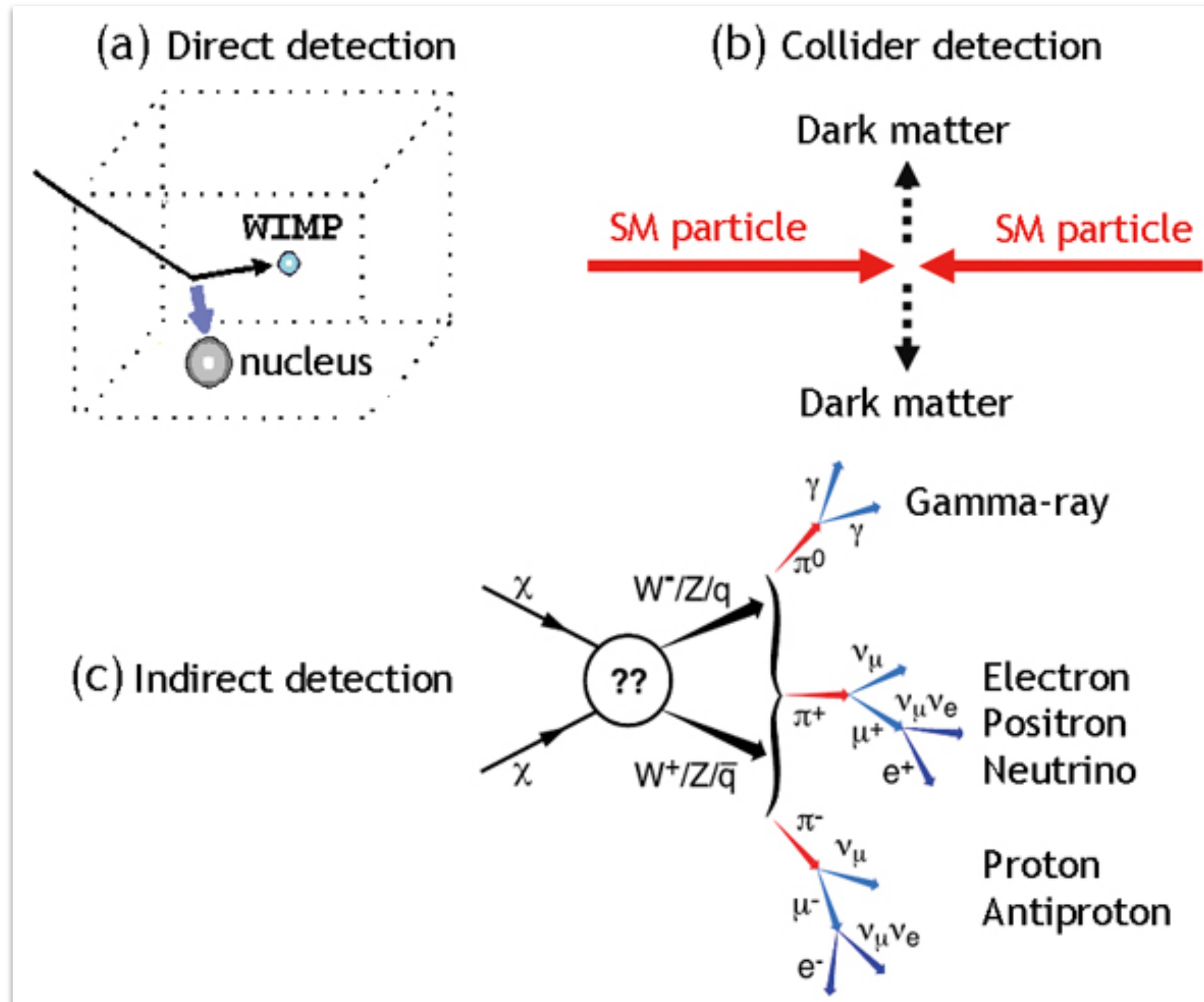
# Dark matter on the mass scale





# Traditional searches for particle dark matter

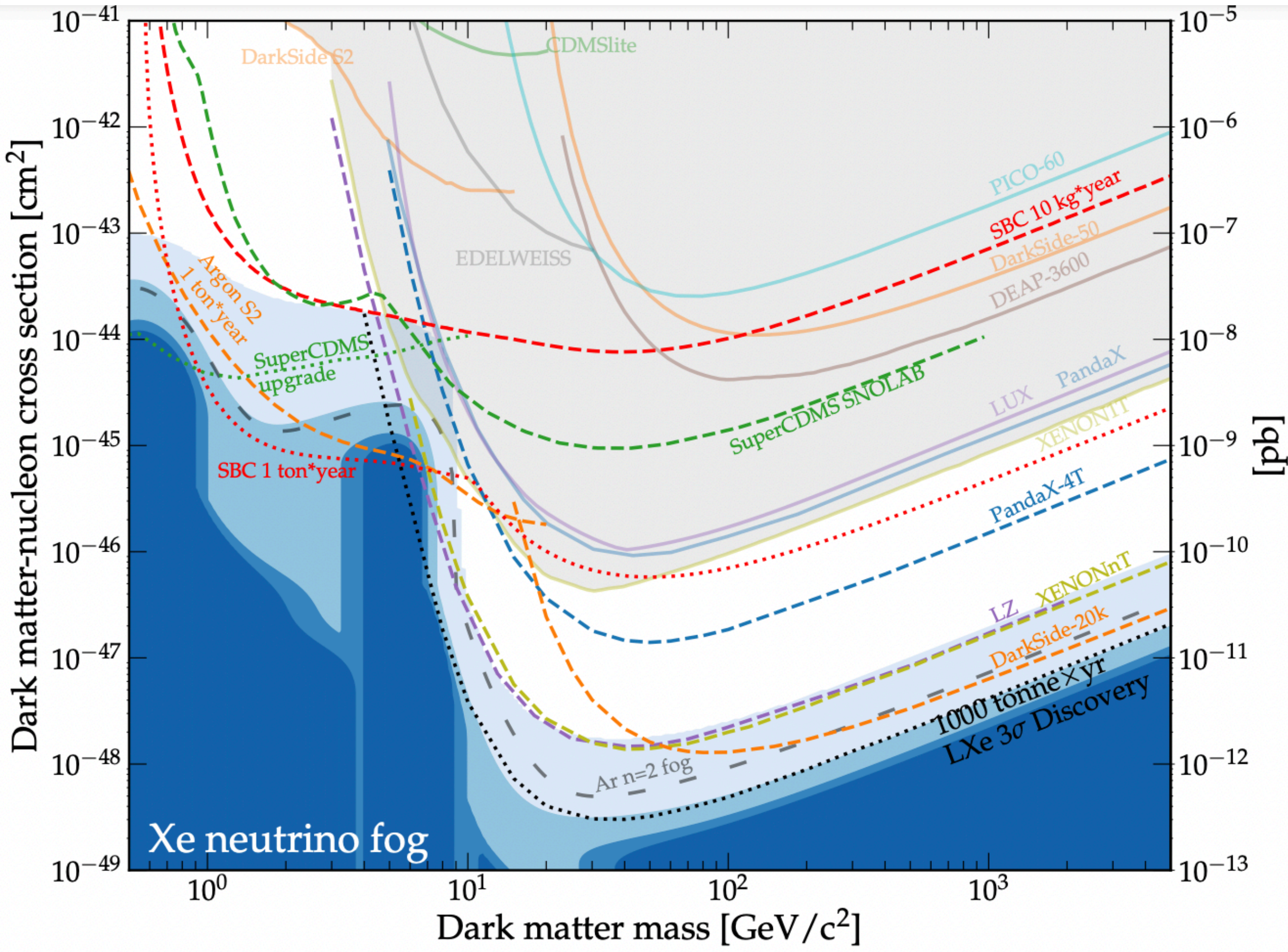
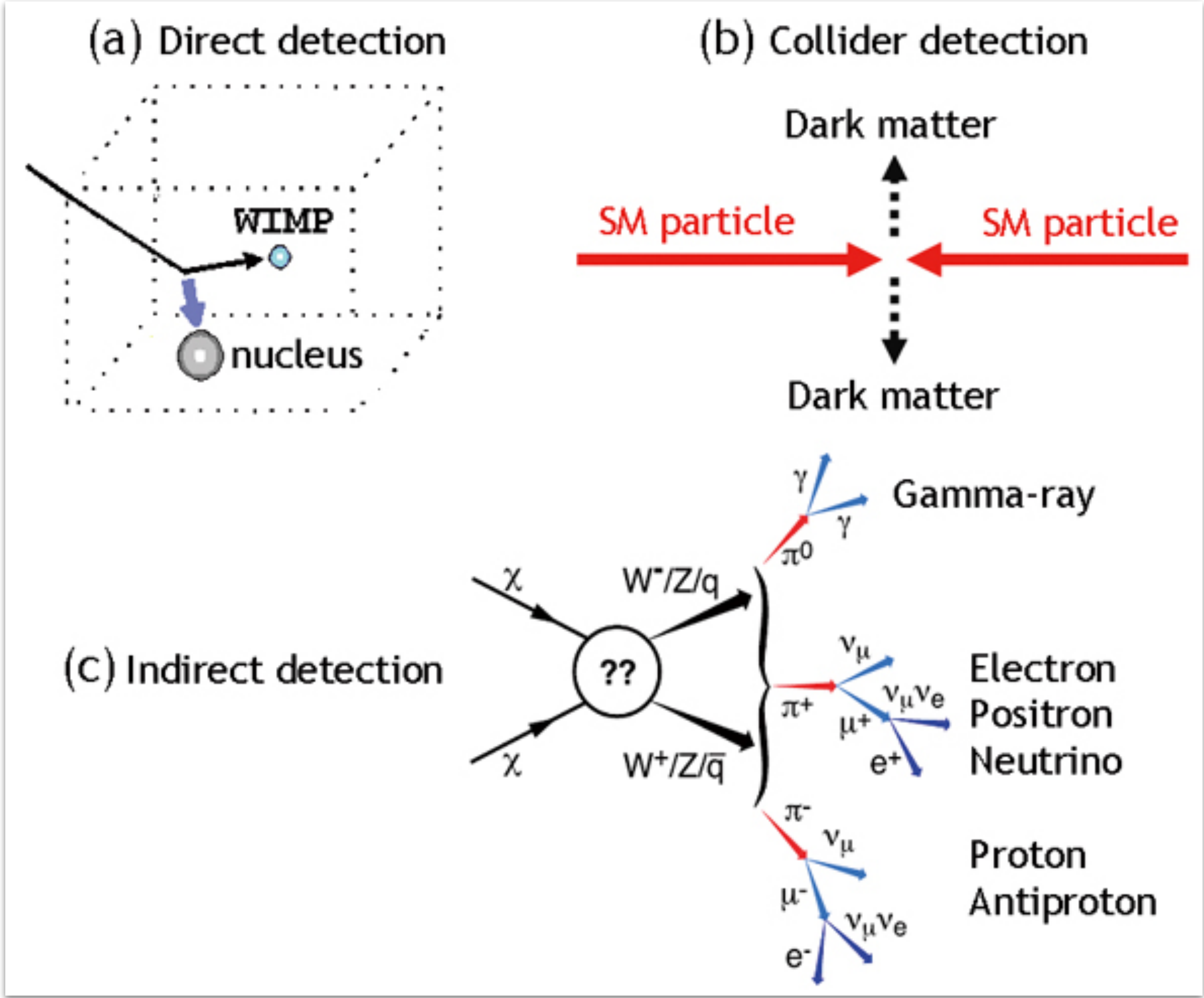
## Thermal WIMPs





# Traditional searches for particle dark matter

## Thermal WIMPs





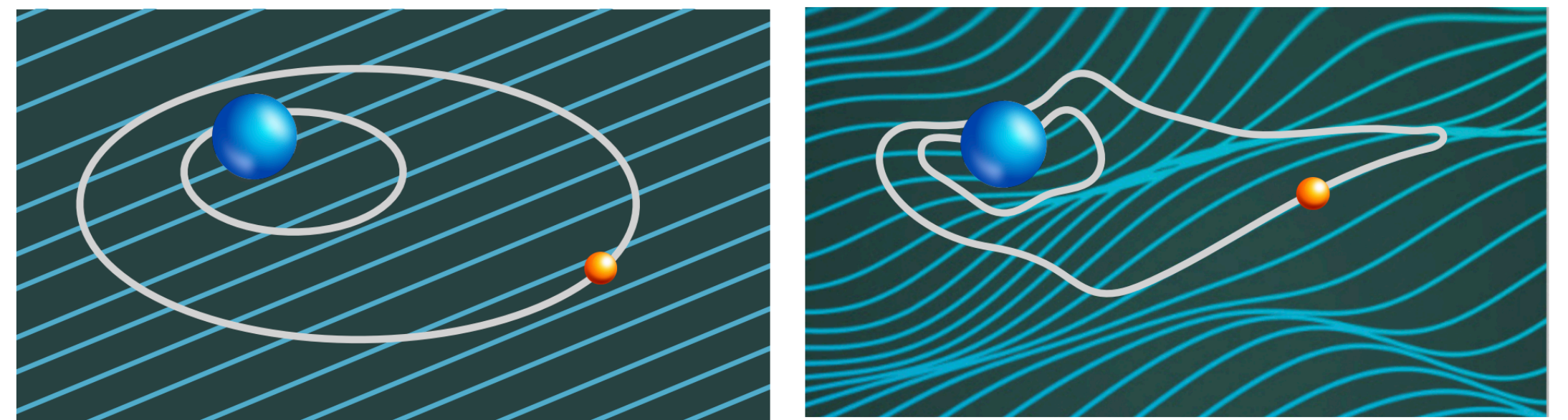
# Wave-like dark matter

fixed by the halo size,  $\lambda \sim \mathcal{O}(\text{kpc})$

classical prescription,  
 $n_\phi (\lambda_{\text{coh}}/2\pi)^3 \gg 1$

- Spin-0 dark matter in the mass range  $\approx 10^{-22} \text{ eV} \lesssim m_\phi \lesssim 1 \text{ eV}$
- When light bosons make up most of dark matter, their number density in galactic halos is high, giving the field a large occupation number — effectively behaving like a classical “wave-like” field.

$$\phi(\vec{x}, t) \approx \frac{\sqrt{2\rho_{\text{DM,local}}}}{m_\phi} \cos\left(m_\phi(t + \underbrace{\vec{\beta} \cdot \vec{x}}_{\phi_0})\right)$$



$|\vec{\beta}| \approx 10^{-3}$  - dark matter velocity,  $\vec{x}$  dependent term amounts to a random phase



# Ultralight dark matter

Low-mass bosonic particles form a coherently oscillating classical field described by :

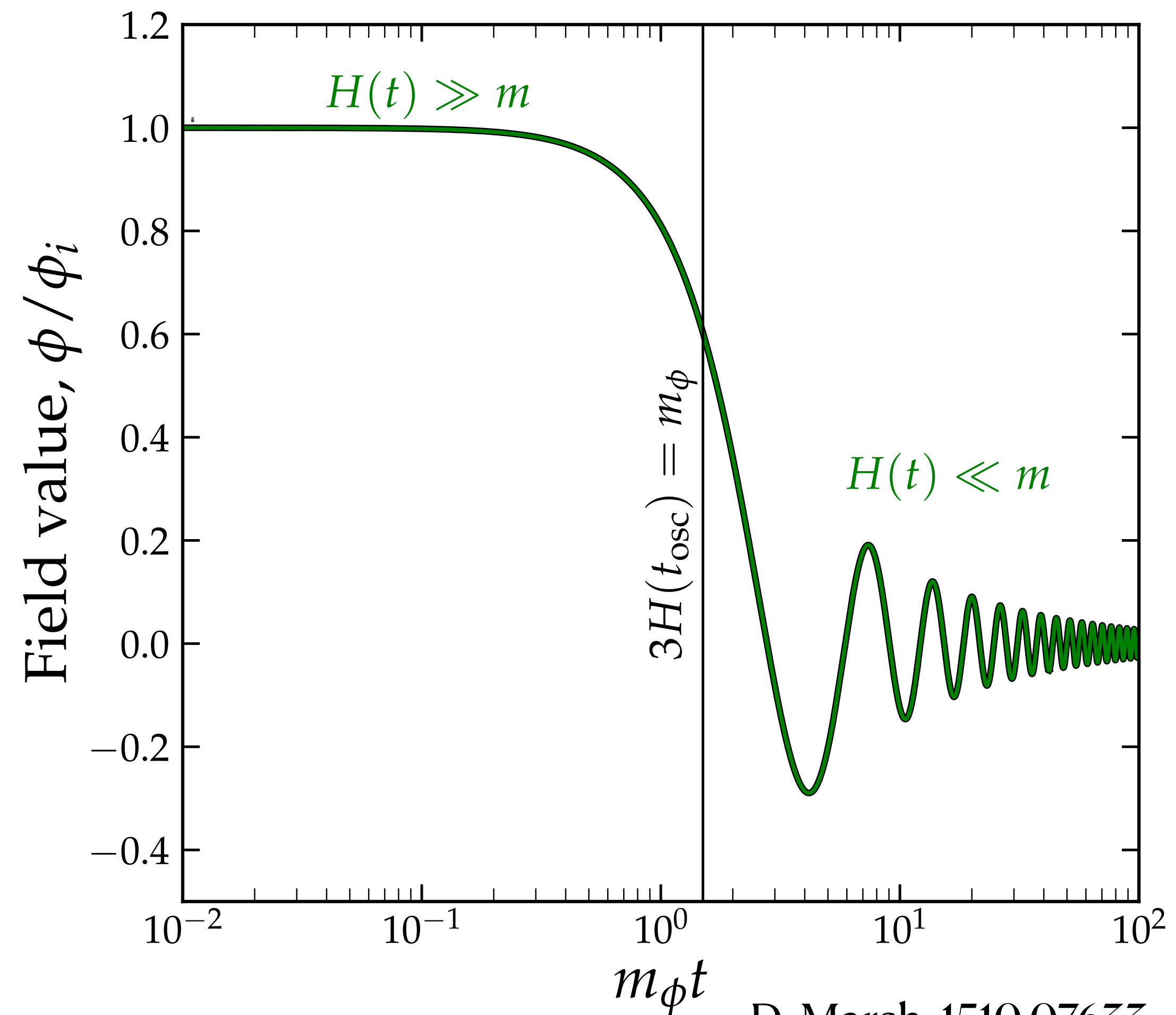
- ✓ Amplitude fixed by dark matter energy density :  $\rho_\phi = \frac{1}{2}m_\phi^2\phi_0^2$  (  $\rho_{\text{DM,local}} \approx 0.4 \text{ GeV/cm}^3$  )
- ✓ The angular frequency determined by the rest mass :  $\omega \sim m_\phi$
- ✓ Small corrections from the kinetic energy :  $\frac{\Delta\omega}{\omega} \sim \frac{\langle v_\phi^2 \rangle}{c^2} \sim 10^{-6}$
- ✓ Coherence time is set by the frequency spread :  $\tau_{\text{coh}} \sim \frac{2\pi}{\Delta\omega} \sim 10^6 T_{\text{osc}}$



# ULDM genesis

- In the early universe, a generic classical field evolves as  $\ddot{\phi} + 3H(t)\dot{\phi} + m_\phi^2\phi = 0$ .
- When  $3H > m_\phi$ , the system behaves like an overdamped oscillator - the field remains static.
- Oscillations start when  $3H \sim m_\phi$  and the field slowly starts rolling towards its potential minimum.
- As the Universe expands,  $H \ll m_\phi$  and the field oscillates and its energy density scales as  $\rho \propto a^{-3}$ , like cold DM.
- Relic density depends on the DM mass and misalignment angle.

## *Misalignment mechanism*



D. Marsh, 1510.07633

C. O'Hare, 2403.17697



# Axions

◎ QCD Axion : a solution to the strong CP problem -  $\theta_{\text{QCD}} \propto a/f_a$  ✓

Peccei Quinn 1972, Weinberg 1978, Wilczek 1978

◎  $m_a \propto \Lambda_{\text{QCD}}^2/f_a$  - mass related to the interactions with SM particles ✓

◎ Pseudo Nambu-Goldstone bosons : has derivative couplings -  $\partial_\mu a \bar{\psi} \gamma_5 \psi / f_a$  ✓

◎ Can constitute a component or all of cold dark matter ✓

$$\mathcal{L} \supset \frac{\alpha_s}{8\pi} \left( \theta + \frac{a}{f_a} \right) G\tilde{G} \quad \Rightarrow \quad \langle a \rangle = -f_a \theta$$

$$m_a f_a \simeq m_\pi f_\pi \sqrt{\frac{m_u m_d}{(m_u + m_d)^2}} \quad \Rightarrow \quad m_a \simeq 5.7 \mu\text{eV} \left( \frac{10^{12} \text{ GeV}}{f_a} \right)$$

$$g_{a\gamma} = \frac{\alpha}{2\pi f_a} (E/N - 1.92) \text{ (KSVZ/DFSZ determine } E/N)$$

$$g_{af} \sim C_f \frac{m_f}{f_a} \text{ from } \partial_\mu a \bar{\psi} \gamma^\mu \gamma_5 \psi / f_a$$



# Axion-like-particles (ALPs)

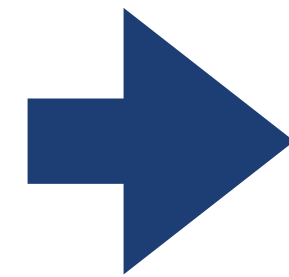
- ◎ ~~QCD Axion : a solution to the strong CP problem -  $\theta_{\text{QCD}} \propto a/f_a$~~  Axion-like particles (ALPs) do not solve strong CP
- ◎  ~~$m_a \propto \Lambda_{\text{QCD}}^2/f_a$  - mass related to the interactions with SM particles~~ ALP mass is a free parameter
- ◎ Pseudo Nambu-Goldstone bosons : has derivative couplings -  $\partial_\mu a \bar{\psi} \gamma_5 \psi / f_a$  ✓
- ◎ Can constitute a component or all of cold dark matter ✓



# ALP interactions at different scales

M. Bauer, SC and G. Rostagni, JHEP 05 (2025) 023

✓ ALPs at the UV scale

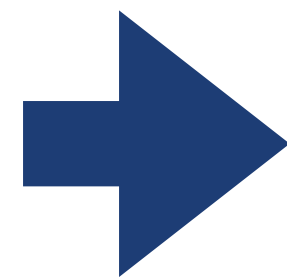


$$\mathcal{L}_{\text{eff}}^{D \leq 5}(\mu > \Lambda_{\text{QCD}}) \ni \frac{\partial^\mu a}{2f} c_{uu} \bar{u} \gamma_\mu \gamma_5 u + \frac{\partial^\mu a}{2f} c_{dd} \bar{d} \gamma_\mu \gamma_5 d + c_{GG} \frac{\alpha_s}{4\pi} \frac{a}{f} G_{\mu\nu} \tilde{G}^{\mu\nu} + \dots$$

✓ RG running

✓ Threshold matching

✓ Chiral Lagrangian



$$\mathcal{L}_{\chi\text{PT}} = \frac{f_\pi^2}{4} \text{tr}[\Sigma m_q(a)^+ + m_q(a) \Sigma^+]$$

$$\Sigma = \exp(i\sqrt{2}\Pi/f_\pi)$$

Quark mass matrix is  
ALP-field dependent !!

$$m_q(a) = e^{-i\kappa_q \frac{a}{f} c_{GG}} m_q e^{-i\kappa_q \frac{a}{f} c_{GG}}$$



# ALP quadratic interactions

$$m_q(a) = e^{-i\kappa_q \frac{a}{f} c_{GG}} m_q e^{-i\kappa_q \frac{a}{f} c_{GG}} \rightarrow m_\pi^2(a) \propto \text{Tr}[m_q(a)] \approx \text{Tr}[m_q] - \frac{a^2}{2f^2} \text{Tr}[\{\kappa_q^2, m_q\}]$$

✓ **Pion mass**  $\rightarrow m_{\pi,\text{eff}}^2(a) = m_\pi^2(1 + \delta_\pi(a)) \rightarrow \delta_\pi(a) = -\frac{c_{GG}^2}{2} \frac{a^2}{f^2} \left(1 - \frac{\Delta_m^2}{\hat{m}^2}\right) + \mathcal{O}(\tau_a^2)$

$$\hat{m} = (m_u + m_d)/2, \Delta_m = (m_u - m_d)/2, \tau_a = m_a^2/m_\pi^2$$

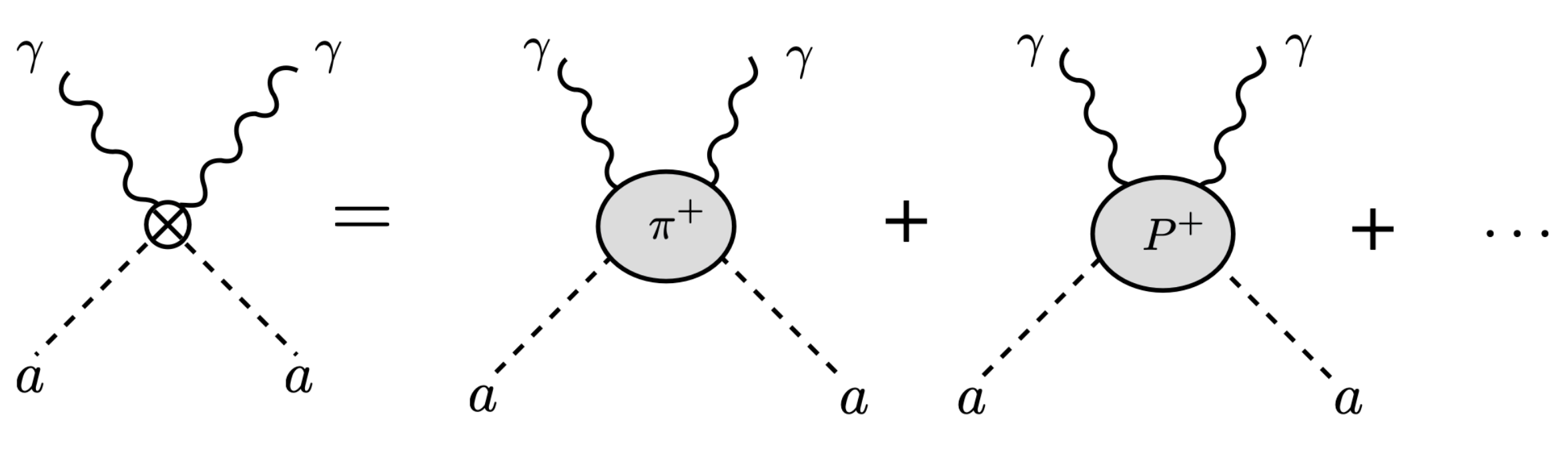
✓ **Nucleon mass**  $\rightarrow \mathcal{L}_{\chi\text{PT}}^{(2)} = c_1 \text{tr}[\chi_+] \bar{N}N + \dots \rightarrow \mathcal{L} \ni 4c_1 m_\pi^2 \delta_\pi(a) \bar{N}N + \dots$

$$c_1 = -1.26 \text{ GeV}^{-2} \text{ (Alarcon et.al, 1210.4450)}$$

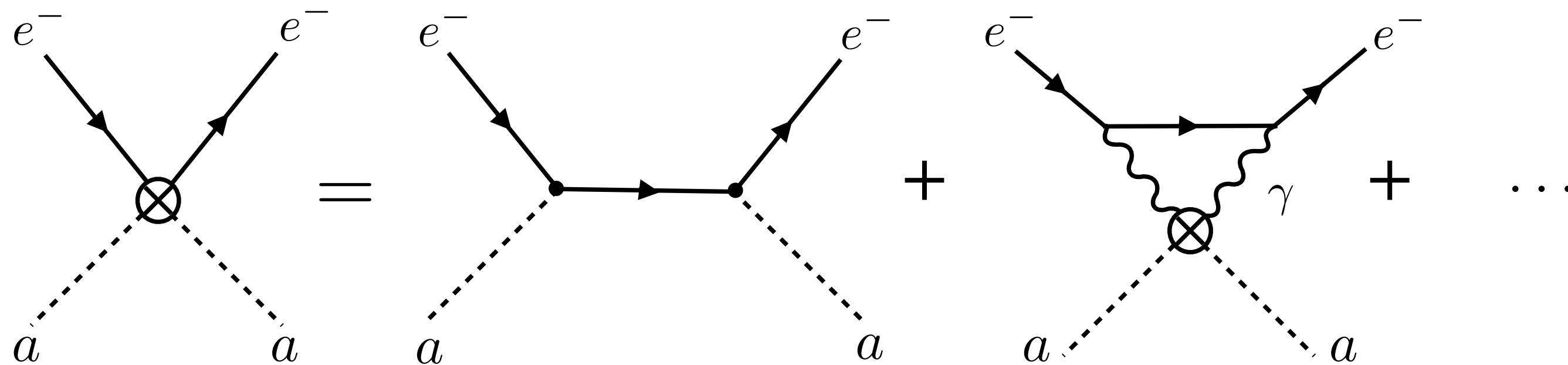
$$\mathcal{L}_{\text{eff}}^{D=6}(\mu \lesssim \Lambda_{\text{QCD}}) = \bar{N} \left( C_N(\mu) \mathbb{1} + C_\delta(\mu) \tau \right) N \frac{a^2}{f^2} + C_E(\mu) \frac{a^2}{f^2} \bar{e}e + C_\gamma(\mu) \frac{a^2}{4f^2} F_{\mu\nu} F^{\mu\nu}$$

At quadratic order in  $f$ , ALPs have scalar interactions described by the dim-6 operators

# Quadratic interactions



$$C_\gamma(\mu) = \frac{\alpha}{24\pi} c_{GG}^2 \left( -1 + 32c_1 \frac{m_\pi^2}{M_N} \right) \left( 1 - \frac{\Delta_m^2}{\hat{m}^2} \right)$$



$$C_E = -m_e \frac{3\alpha}{4\pi} C_\gamma \ln \frac{m_\pi^2}{m_e^2}$$



# Shifts in fundamental constants

$$\mathcal{L}_{\text{eff}}^{D=6}(\mu \lesssim \Lambda_{\text{QCD}}) = \bar{N} \left( C_N(\mu) \mathbb{I} + C_\delta(\mu) \tau \right) N \frac{a^2}{f^2} + C_E(\mu) \frac{a^2}{f^2} \bar{e} e + C_\gamma(\mu) \frac{a^2}{4f^2} F_{\mu\nu} F^{\mu\nu}$$

In the oscillating dark matter background, the low-energy quadratic Lagrangian induces a time-dependent component in the following fundamental constants :

$$\checkmark \quad \alpha^{\text{eff}}(a) = \left( 1 + \delta_\alpha(a) \right) \alpha \quad \text{with} \quad \delta_\alpha(a) = \frac{1}{12\pi} \left( 1 - 32c_1 \frac{m_\pi^2}{M_N} \right) \delta_\pi(a)$$

$$\checkmark \quad m_e^{\text{eff}}(a) = m_e \left( 1 + \delta_e(a) \right) \quad \text{with} \quad \delta_e(a) = \frac{3\alpha}{4\pi} C_\gamma \frac{a^2}{f^2} \ln \frac{m_\pi^2}{m_e^2}$$

**So, the building blocks of atoms oscillate in time!!!**

$$\checkmark \quad M_N(a) = M_N \left( 1 + \delta_N(a) \right) \quad \text{with} \quad \delta_N(a) = -4c_1 \frac{m_\pi^2}{M_N} \delta_\pi(a)$$

## Context Summary

- Ultralight dark matter is a *coherent oscillating field*, not individual particles.
- Produced by misalignment; QCD axion is the classic case, ALPs generalize with free mass–coupling.
- At low energies, couplings mix into pions, nucleons, electrons → shifts fundamental constants.
- Net effect: *time-varying constants* like  $m_e$ ,  $m_N$ , and  $\alpha$ .

## Next Steps:

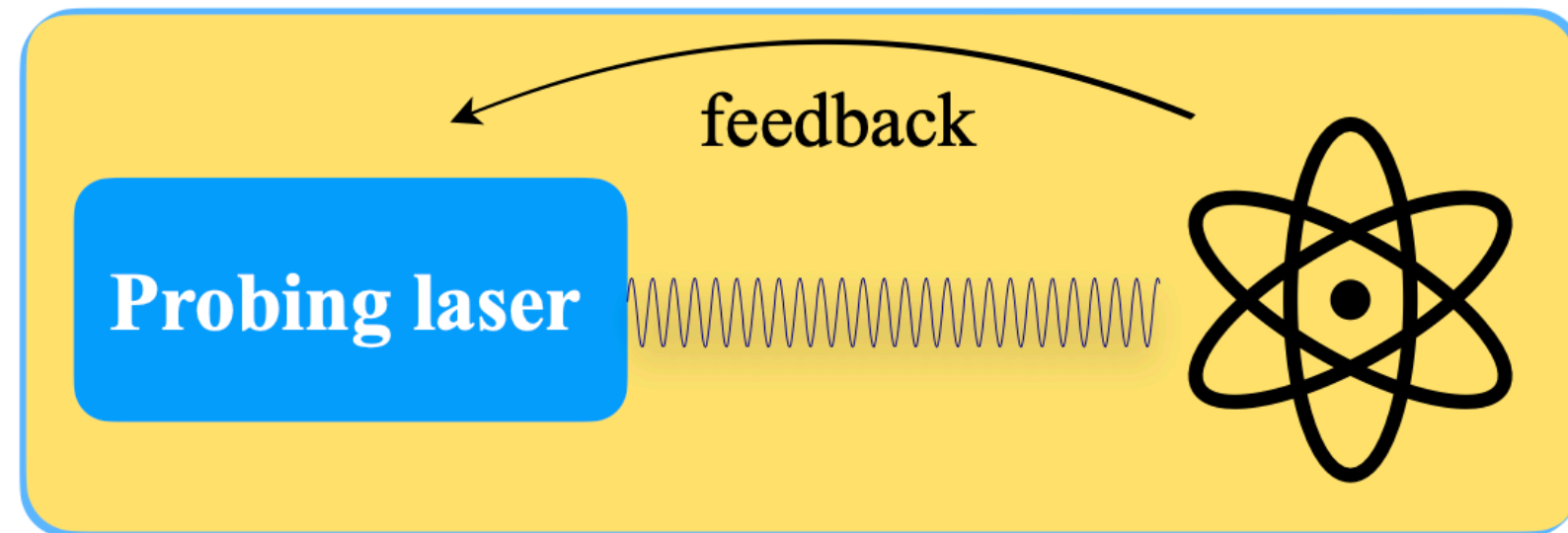
So that's the theory picture: dark matter makes the building blocks of atoms oscillate. The next step is: how do we actually see those oscillations in the lab?



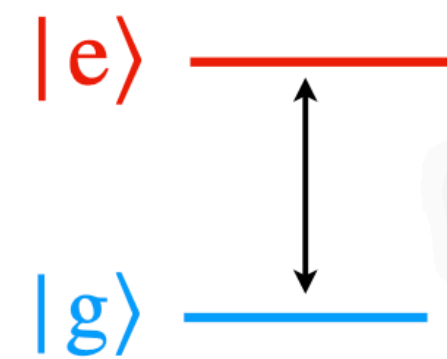
# Phenomenology

# Atomic Clocks

## Basic components



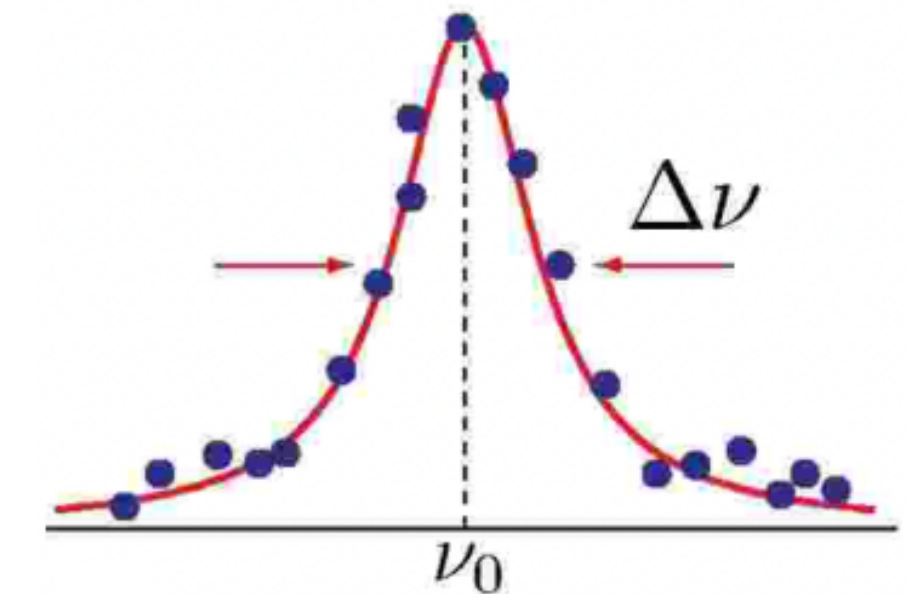
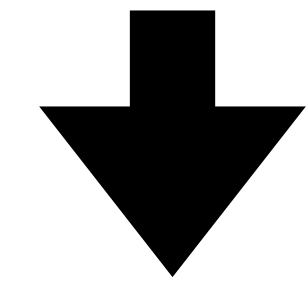
## Clock transition



$$\text{[wavy line]} = h\nu_{\text{output}}$$

## Measured\* radiation

laser/microwave is tuned in resonance with the transition



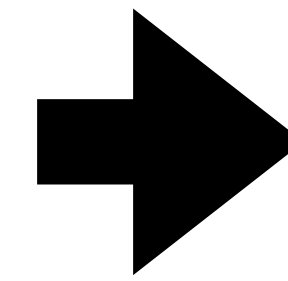
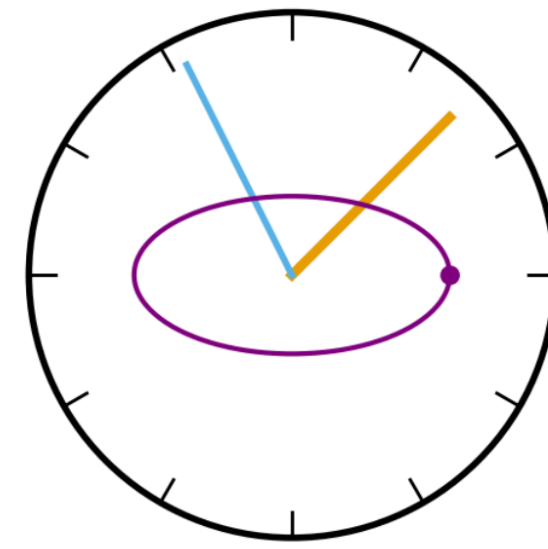
$$r_{\text{observable}} = \frac{\nu_1}{\nu_2}$$

Different transitions of same system  
or distinct systems

- Quantum clocks, operate by comparing the frequency ratios of different atomic, vibrational and nuclear transitions.
- Clock frequencies rely on the frequencies of spectral lines in these transitions. Therefore, a fractional change in the spectra brings in a shift in the clock frequency
- Clock searches are naturally broadband, with mass range depending on the total measurement time and specifics of the clock operation protocols



# Clock sampling



- ⦿ Ultra-stable
- ⦿ Coherent

**Allan deviation** gives the measure of stability :  $\sigma_y(\tau) = \sqrt{\frac{1}{2} \langle (y_{i+1} - y_i)^2 \rangle}$

where  $y_i$  = average fractional frequency over time window  $\tau$ .

**White (thermal) noise:**

$$\sigma_y(\tau) \propto \frac{1}{\sqrt{\tau}}$$

→ averages down with longer time.

**Flicker noise:**

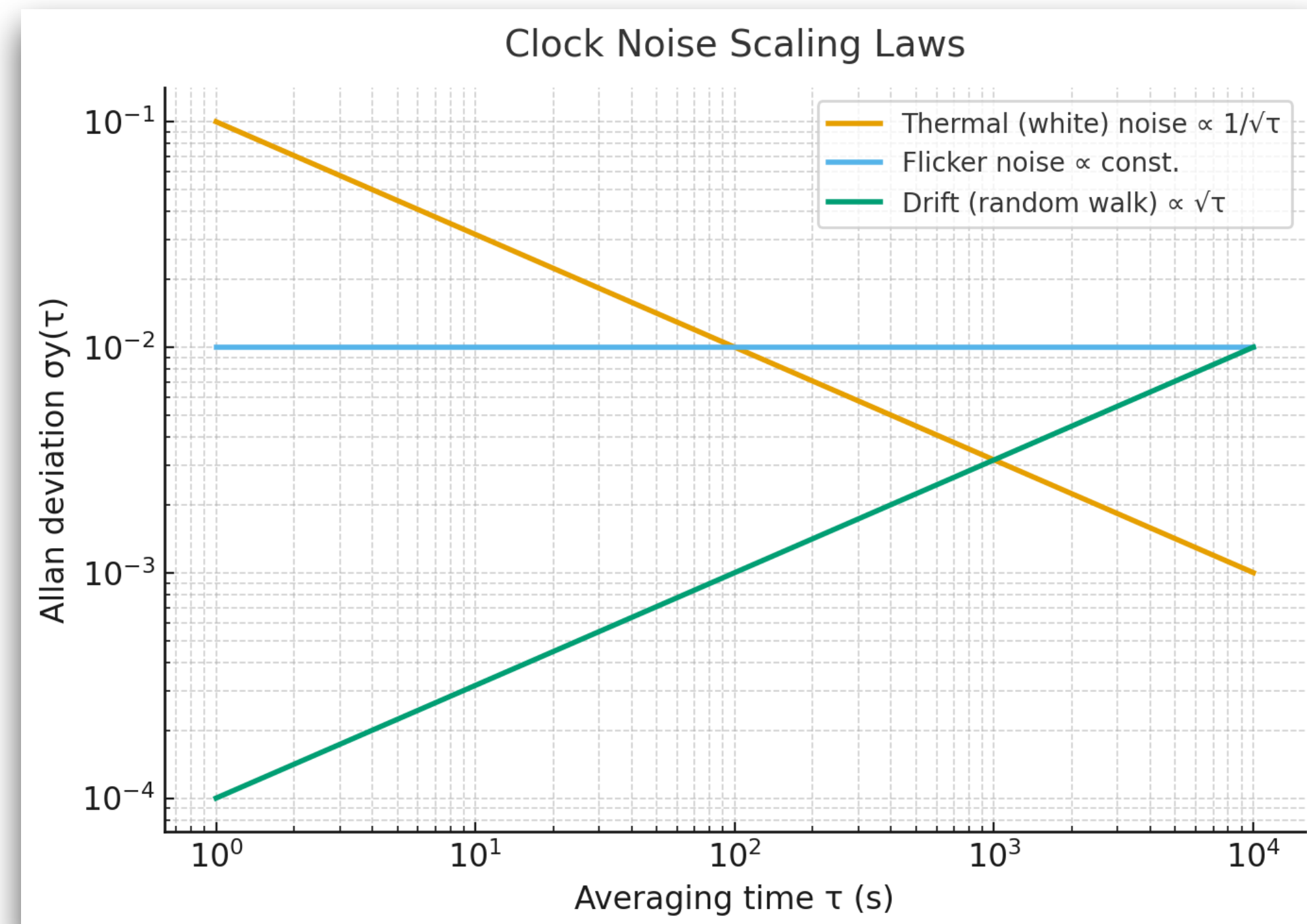
$$\sigma_y(\tau) \approx \text{const.}$$

→ flat, doesn't improve with averaging.

**Drift (random walk):**

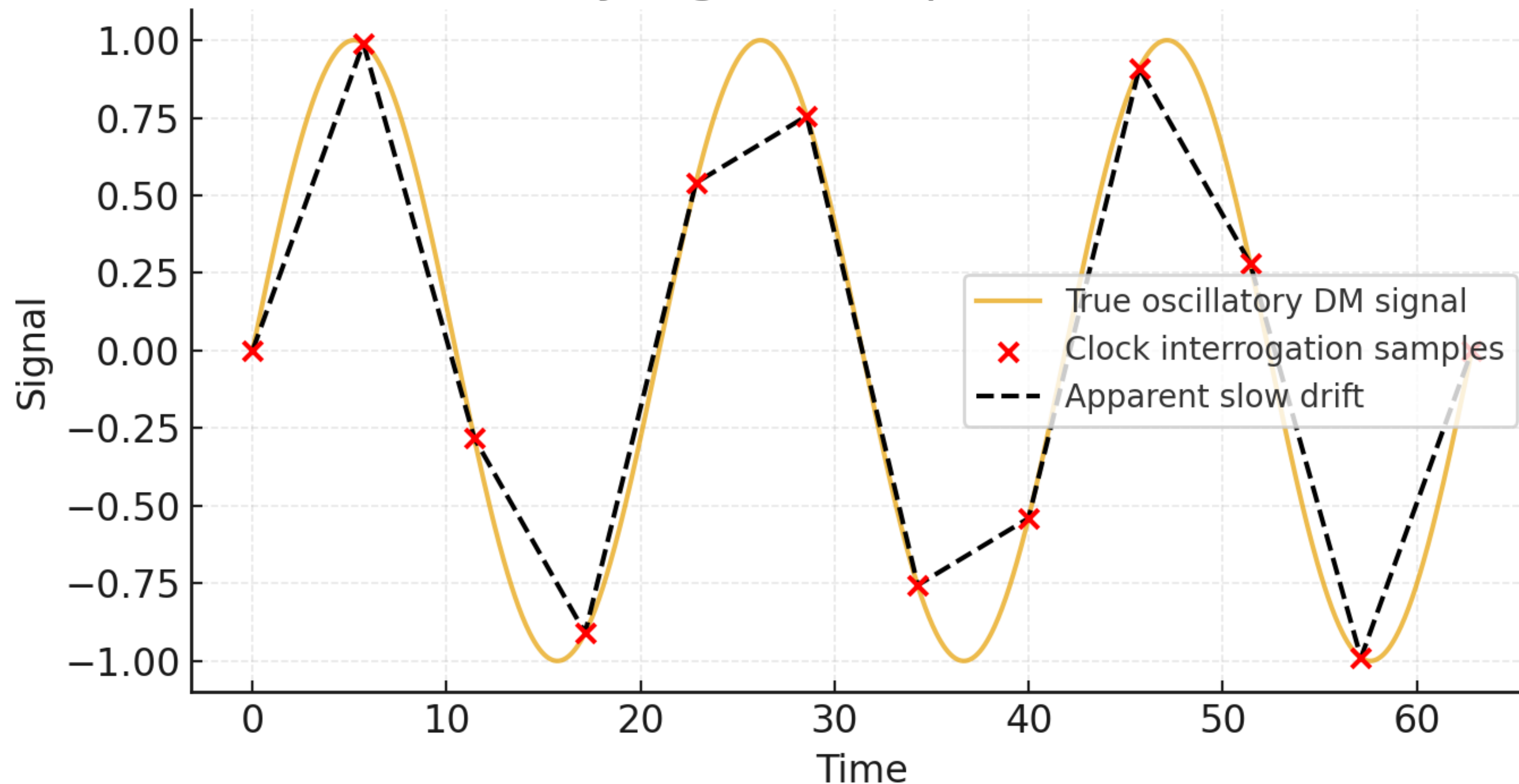
$$\sigma_y(\tau) \propto \sqrt{\tau}$$

→ gets worse the longer you run.



# One clock : drift can be systematics or signal

Oscillatory Signal Sampled as Slow Drift



- For Rb fountains the interrogation time is ~10–20 ms, and for Cs ~50 ms.
- The typical period of oscillation ~ 2 months

**Compare one clock, never sure what's on the table !!!**



# Two co-located clocks

- ◎ **Direct frequency comparison:** best way to probe fundamental constant variations.
- ◎ **Shared environment:** temperature, vibrations, and magnetic field noise mostly cancel.
- ◎ **Systematics cancel only partially:** species-specific or setup-dependent effects remain.
- ◎ **High coherence:** since both clocks see the same environment, long interrogation times are possible.
- ◎ **Ideal for stability benchmarks:** co-located ratios define the state of the art in precision metrology.

# Clock comparison

- ✓ The frequency ratio of atomic transitions in two different atomic clocks  $A$  and  $B$  is parametrised as:

Difference in the sensitivity coefficients

$$\nu_{A/B} \propto \alpha^{k_\alpha} \left( \frac{m_e}{m_p} \right)^{k_e} \left( \frac{m_q}{\Lambda_{\text{QCD}}} \right)^{k_q}$$

- ✓ To obtain a signal in the clock comparison, the sensitivity coefficients of the two systems must be different.



- The observable is the fractional variation in the frequency ratio of  $A$  and  $B$  :

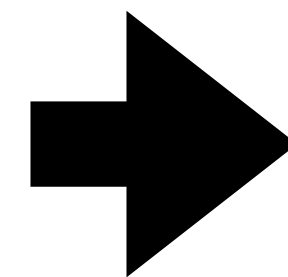
$$\frac{\delta\nu_{A/B}}{\nu_{A/B}} = k_\alpha \frac{\delta\alpha}{\alpha} + k_e \left( \frac{\delta m_e}{m_e} - \frac{\delta m_p}{m_p} \right) + k_q \left( \frac{\delta m_q}{m_q} - \frac{\delta \Lambda_{\text{QCD}}}{\Lambda_{\text{QCD}}} \right)$$

$$\frac{\delta\nu_{A/B}}{\nu_{A/B}} = k_\alpha \delta_\alpha(a) + k_e \delta_e(a) - (k_e + 2k_q) \delta_p(a) + k_q \delta_\pi(a)$$

- Microwave clocks are based on hyperfine transitions - frequencies of a few GHz. Primarily sensitive to the variations in  $\alpha$  and  $m_e/m_p$ .
- Optical clocks are based on transitions between different electronic levels - frequencies of  $\sim \mathcal{O}(10^{15})$  Hz. Sensitive to variations in  $\alpha$ .

In the oscillating dark matter background,

$$\frac{\delta\nu_{A/B}}{\nu_{A/B}} \propto a^2 = \frac{2\rho_{\text{DM}}}{m_a^2} \cos^2 m_a t = \frac{\rho_{\text{DM}}}{m_a^2} (1 + \cos 2m_a t)$$



Signal is obtained when  
Clock frequency  $\omega \simeq 2m_a$

## Microwave clocks

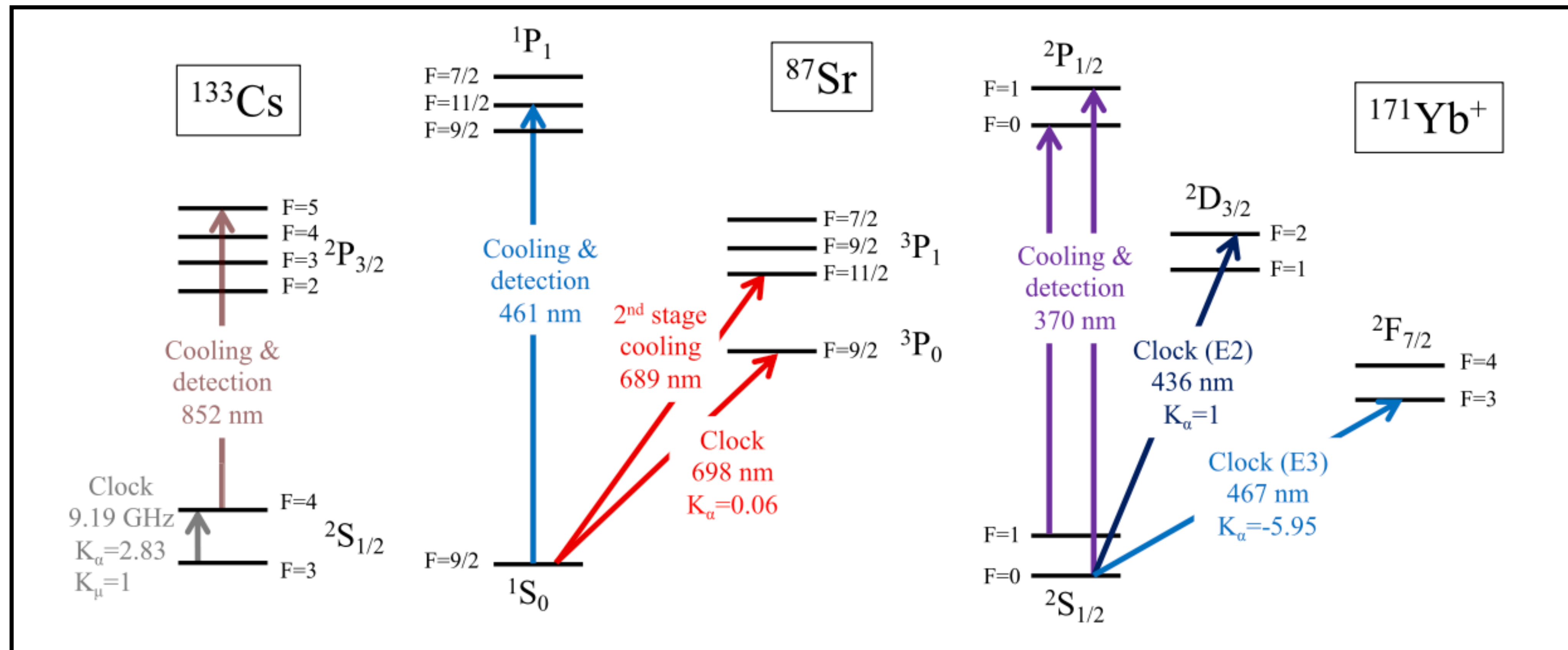
~ GHz frequencies.  
Longer integration time.  
Fractional uncertainty ~  $10^{-15}$   
Rb/Cs

$$\text{clock stability} \propto \nu_0 / \Delta\nu$$

**narrow linewidth gives higher stability**

## Optical clocks

~ THz frequencies.  
Fractional uncertainty ~  $10^{-17}$   
Yb, Al, Hg, Sr ion clocks





# Different clock comparisons

Sensitive to different fundamental constants

Hyperfine frequencies :

$$\nu \propto \alpha^4 m_e^2 / m_p F_{\text{MW}}(\alpha)$$

Optical frequencies :

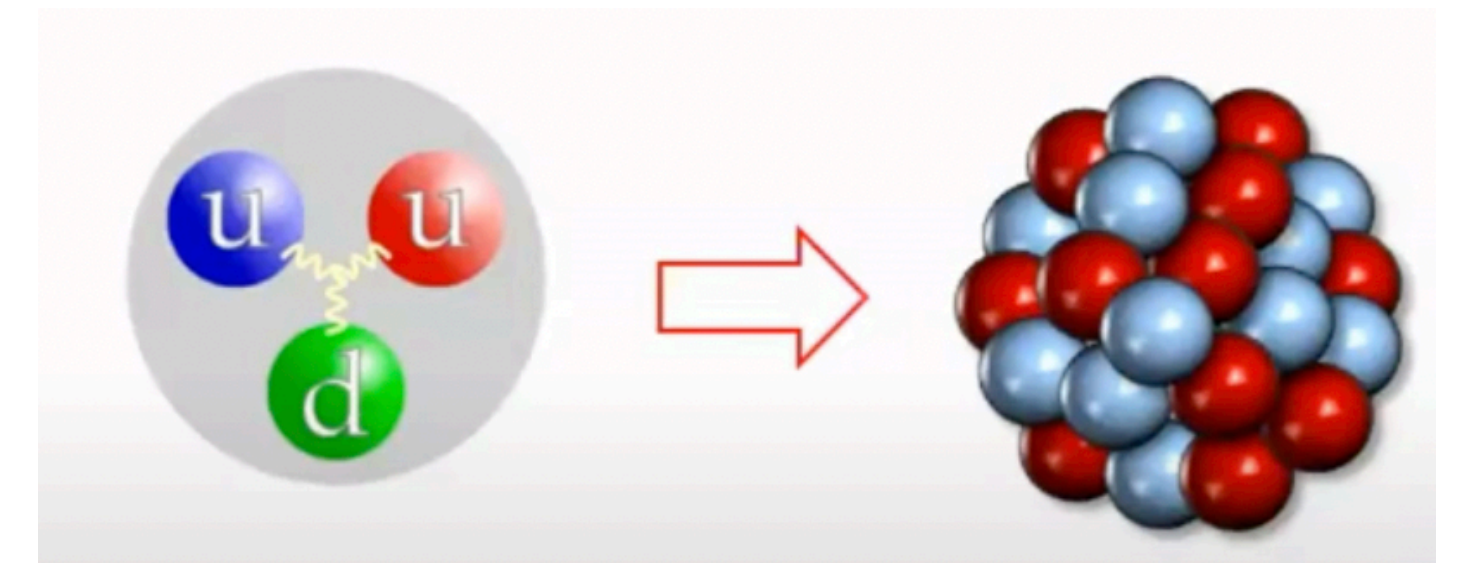
$$\nu \propto \alpha^2 m_e F_o(\alpha)$$

- *Two microwave clocks : Rb/Cs* - transitions between different hyperfine levels in the two ground state atoms  $^{87}\text{Rb}$  and  $^{133}\text{Cs}$  . Sensitive to very low frequencies corresponding to ALP mass  $\sim 10^{-20}$  eV and below due to the long time-span of the experiment.
- *Two optical clocks : BACON* –  $\text{Al}^+/\text{Yb}$ ,  $\text{Yb}/\text{Sr}$  and  $\text{Al}^+/\text{Hg}^+$  frequency comparisons.
  - $\text{Yb}^+ E_3/E_2$  : comparison between the electric-octupole transition ( $E_3$ ) and the electric-dipole transition ( $E_2$ ) of  $^{171}\text{Yb}^+$  ion.
  - $\text{Yb}^+ E_3/\text{Sr}$  : frequency ratio between the  $E_3$  transition in  $^{171}\text{Yb}^+$  to a transition in the optical lattice clock  $^{87}\text{Sr}$  is measured.
- *Optical and microwave clock comparisons : Yb/Cs* – all three sensitivity coefficients  $k_\alpha$ ,  $k_e$  and  $k_q$  are non-zero, which makes it particularly sensitive to variations in  $m_e$ .

# New developments in optical clocks

The QCD-interactions of the oscillating dark matter field give rise to oscillations in the nuclear charge radius. In heavy atoms like  $^{171}\text{Yb}^+$ , there is a large contribution from the “field-shift energy” in the total electronic energy, since  $E_{\text{FS}} \simeq K_{\text{FS}} \langle r_N^2 \rangle \propto A^{2/3}$ .

$$\frac{\Delta(\nu_a/\nu_b)}{(\nu_a/\nu_b)} = K_{a,b} \frac{\Delta \langle r_N^2 \rangle}{\langle r_N^2 \rangle} \quad K_{a,b} \equiv \frac{K_{\text{FS}}^{\nu_a} \langle r_N^2 \rangle}{\nu_a} - \frac{K_{\text{FS}}^{\nu_b} \langle r_N^2 \rangle}{\nu_b}$$



courtesy : M. Safronova

$\langle r_N^2 \rangle$  is dominated by the distribution of protons within the nucleus and the inter-nucleon distance, which are sensitive to pion decay constant, pion mass and pion-exchange processes.

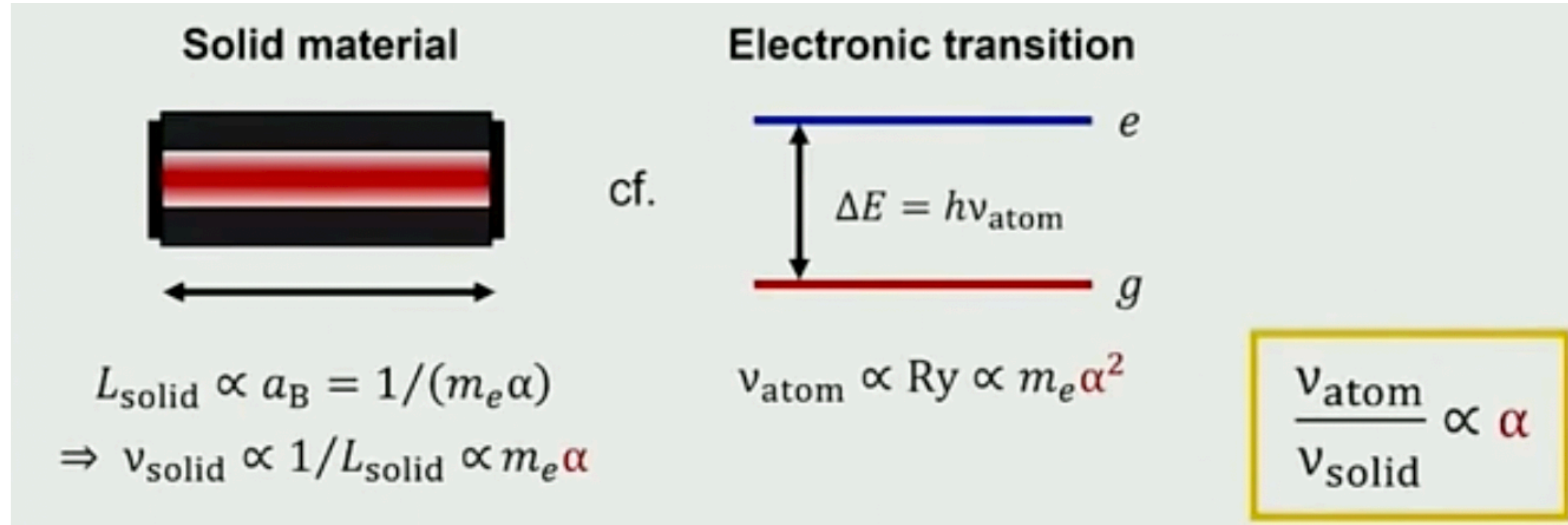
$$\frac{\Delta \langle r_N^2 \rangle}{\langle r_N^2 \rangle} \approx \alpha \frac{\Delta f_\pi}{f_\pi} + \beta \frac{\Delta m_\pi^2}{m_\pi^2} \approx \alpha \frac{\Delta \Lambda_{\text{QCD}}}{\Lambda_{\text{QCD}}} + \beta \frac{\Delta m_\pi^2}{m_\pi^2}$$

**sensitivity improved by several orders  
compared to BACON clocks!!**

$$\begin{aligned} & \text{Yb}^+ E_3/E_2 \\ & (4f^{14}6s)^2S_{1/2} - (4f^{13}6s)^2F_{1/2} (E_3) \\ & (4f^{14}6s)^2S_{1/2} - (4f^{14}5d)^2D_{3/2} (E_2) \\ & \text{Banerjee et.al, arXiv:2301.10784} \end{aligned}$$



# Optical Cavities



courtesy : Y. Stadnik

- The FC variations in the oscillating DM background induces a change in the length of solid objects such as optical cavities due to variations in Bohr radius.
- The fractional change in the cavity length causes a change in the frequency of the eigenmodes of the cavity, which scales as the inverse of the cavity length.
- The cavity reference frequency,  $\nu_c \propto \alpha m_e$  is compared to the atomic transition frequencies in the clocks or other cavities in the optical/microwave domain.



# Clock-cavity & cavity-cavity comparisons

- **Sr/Si** : frequency comparison between a Si optical cavity and a  $^{87}\text{Sr}$  optical lattice clock. Only sensitive to the variation in the fine-structure constant, due to  $\nu_{\text{Sr}} \propto \alpha^{2.06} m_e$ . Operates in the optical domain with higher frequency stability and provides the strongest limits in the range  $m_a \approx 10^{-17} - 2 \times 10^{-16}$  eV.

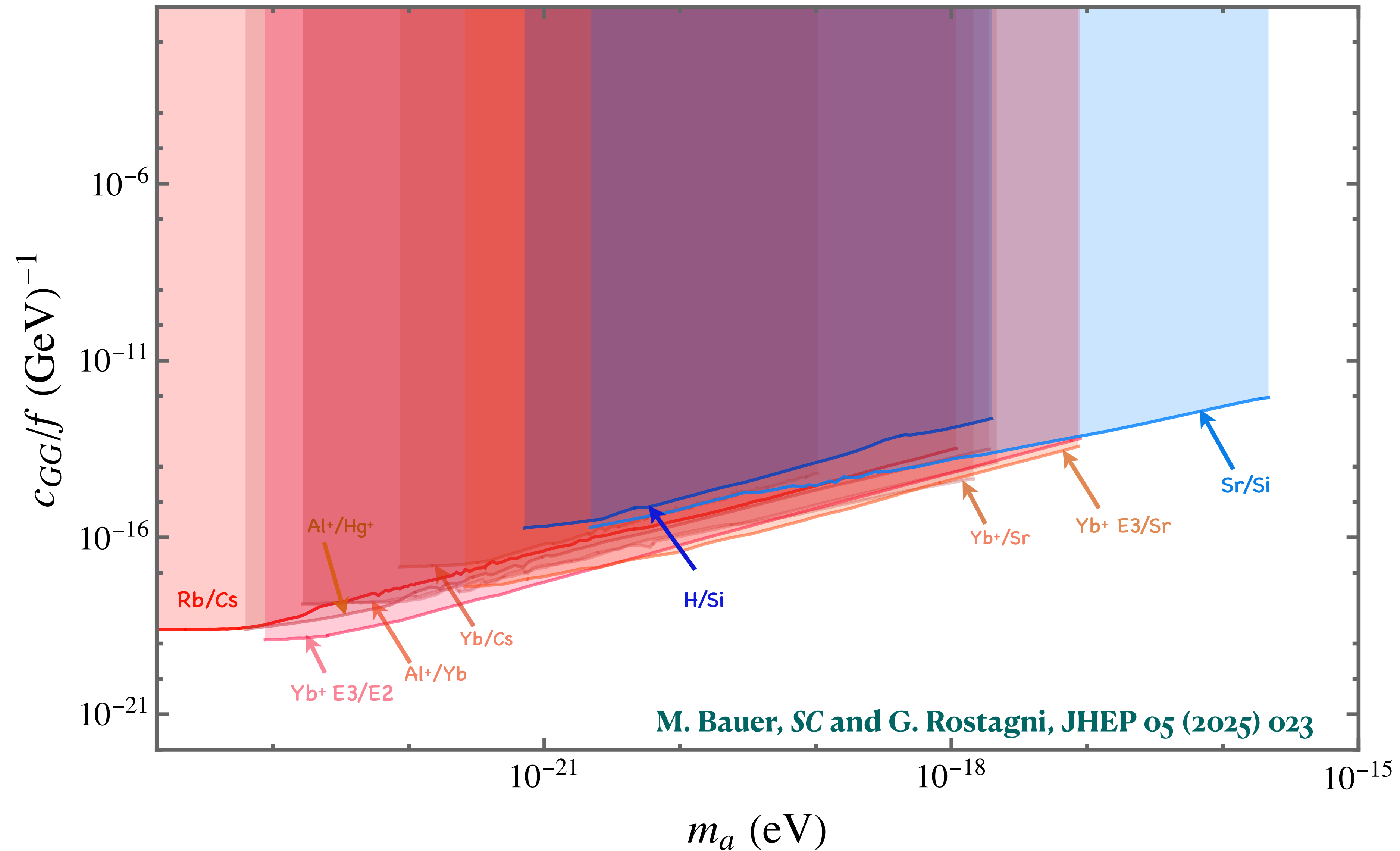
*Kennedy et. al, Phys. Rev. Lett. 125, 201302 (2020)*

- **H/Si** : comparison of the reference frequency of a Si cavity and an H maser. Sensitive to both  $\alpha$  and  $m_e$  variation because the hyperfine transition frequency of H maser shows a different functional dependence on  $m_e$  compared to the cavity frequency -  $\nu_H \propto \alpha^4 m_e^2$ . Operates in the microwave domain.

- **Cs/D2** : Larger ALP mass is constrained by comparing the measurements of electronic transitions between two states of  $^{133}\text{Cs}$  against a laser cavity. Sensitive to FC variations between the acoustic cut-off frequency of the cavity resonator and the frequency of the natural line width of the excited state. Constrains ALPs in the range  $m_a \approx 4.6 \times 10^{-11} - 10^{-7}$  eV.

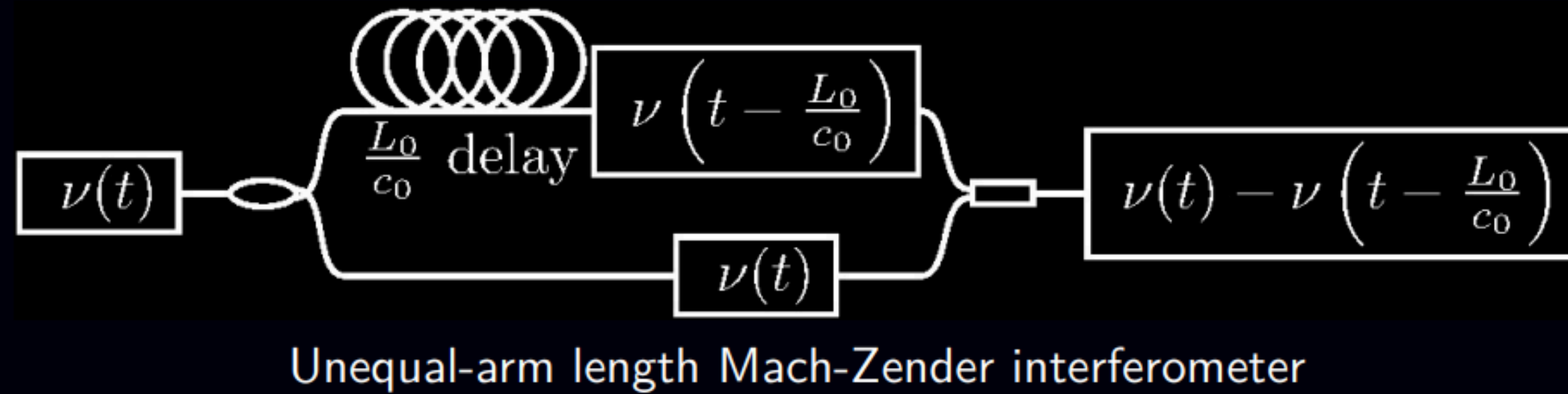
*Antypas et. al, Phys. Rev. Lett. 123, 141102, Tretiak et. al, Phys. Rev. Lett. 129 (2022)*

# Coverage@Low frequencies



# Unequal time-delay cavities

"DAMNED" allows to compare an ultrastable cavity to itself in the past.

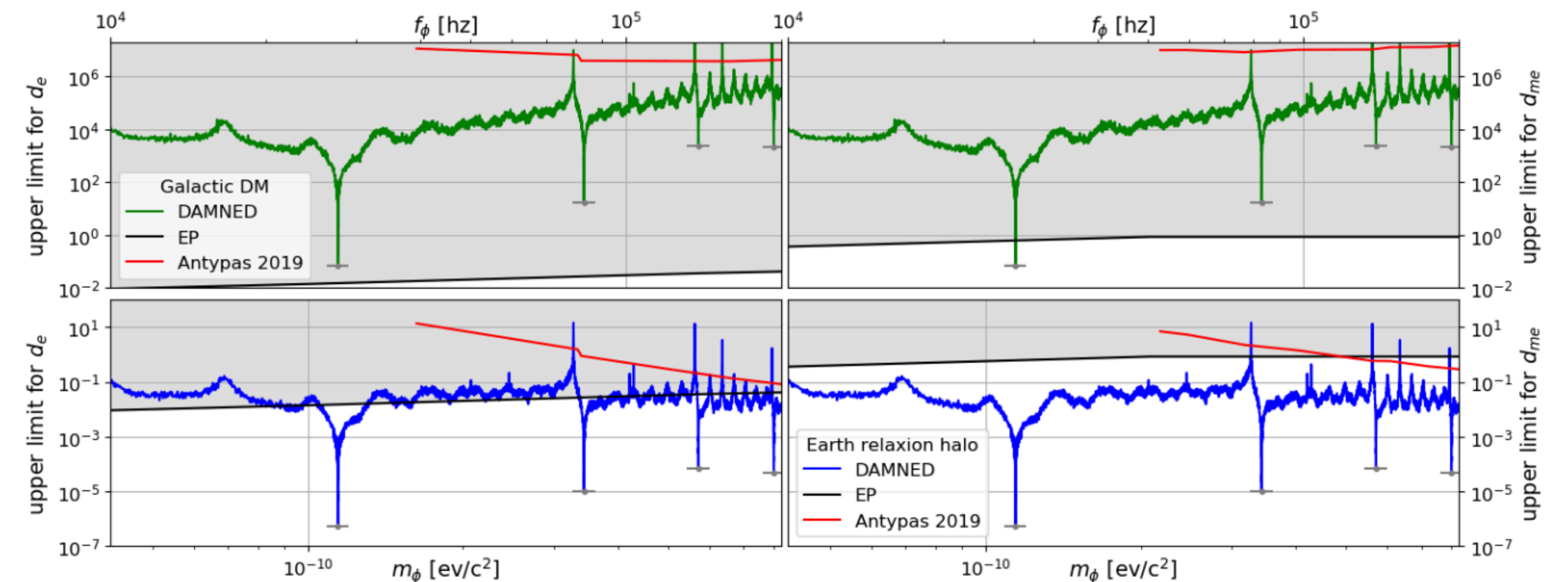


Phase difference between the delayed and non delayed signals

$$\Delta\Phi(t) = \omega_0 T_0 + \omega_0 \int_{t-T_0}^t \left( \frac{\Delta T(t')}{T_0} + \frac{\Delta\omega(t')}{\omega_0} \right) dt' + \omega_0 T_0 \left( \frac{\delta T}{T_0} + \frac{\delta\omega}{\omega_0} \right) \sin \left( \omega_\varphi t - \omega_\varphi \frac{T_0}{2} \right) \text{sinc} \left( \omega_\varphi \frac{T_0}{2} \right)$$

**Color code**  
 NOMINAL VALUE  
 NOISE  
 DARK MATTER EFFECT

- **Pros** : single setup, higher frequency
- **Cons**: sensitivity

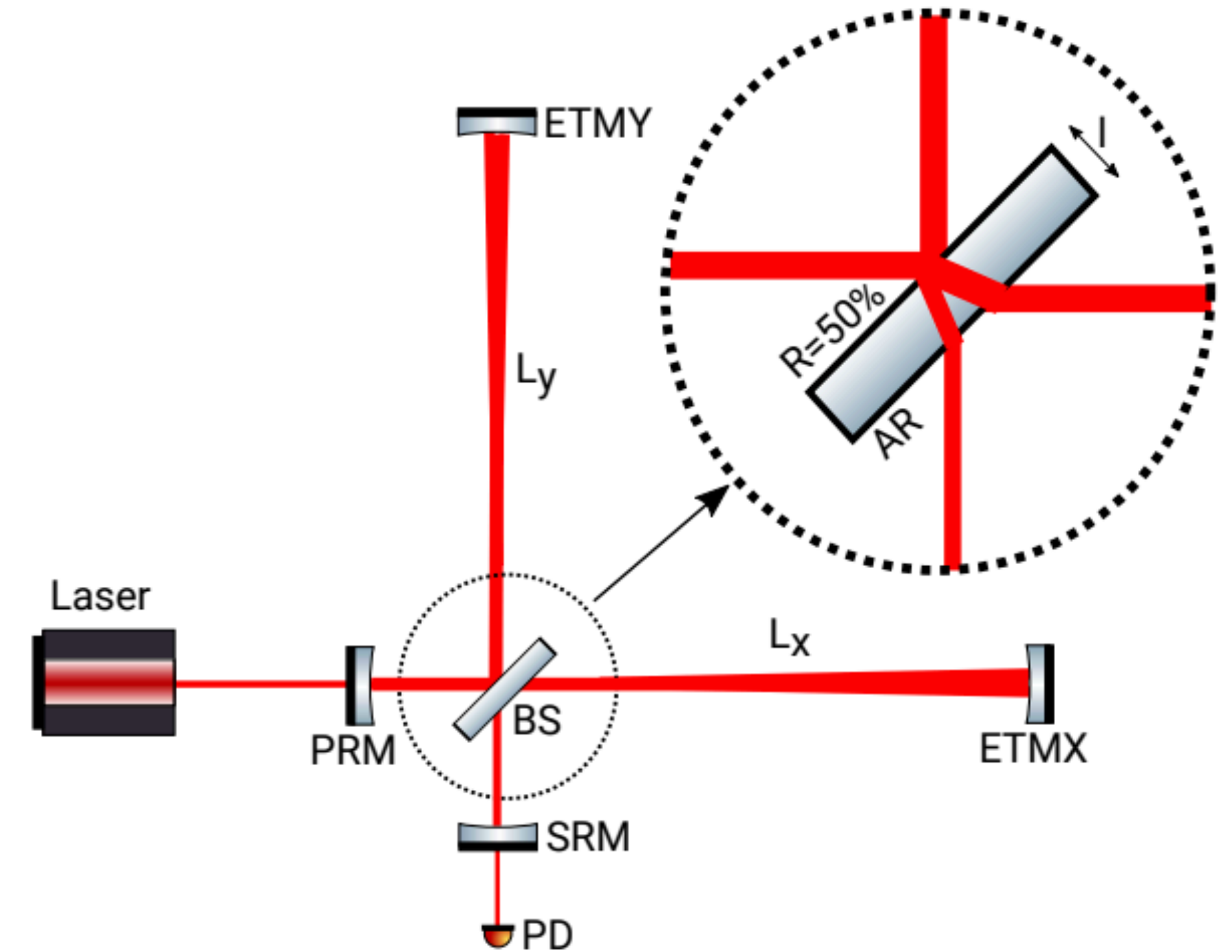


Courtesy : Etienne SAVALLE (DAMNED collaboration)



# Optical interferometers

- A two-arm laser interferometer is typically used to detect small changes in the difference of the optical path lengths in the two arms of the interferometer.
- The two arms of an interferometer are practically equal in terms of optical path length. However, the beam splitter can create a geometric asymmetry. The beam-splitter and arm mirrors of an interferometer, if freely suspended, can produce differential optical-path length variations due to changes in the fundamental constants.
- A freely-suspended beam-splitter would experience time-varying size changes about its centre-of-mass, thus shifting back-and-forth the main reflecting surface that splits and recombines the laser beam would create the phase difference, hence the signal.



H. Grote1 *et. al*, [arXiv: 1906.06193]

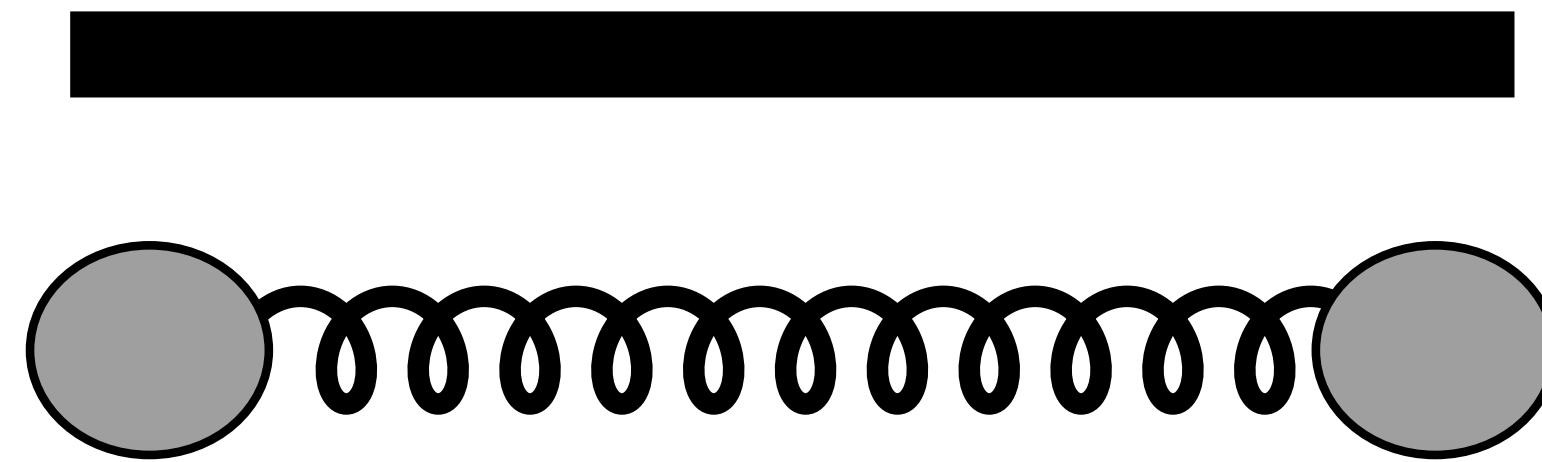
$$\frac{\delta l}{l} = - \left( \frac{\delta \alpha}{\alpha} + \frac{\delta m_e}{m_e} \right)$$

$$\frac{\delta n}{n} = -5 \times 10^{-3} \left( 2 \frac{\delta \alpha}{\alpha} + \frac{\delta m_e}{m_e} \right)$$

$$\delta(L_x - L_y) = \sqrt{2} \left[ \left( n - \frac{1}{2} \right) \delta l + l \delta n \right] \approx n l [\delta_\alpha(a) + \delta_e(a)]$$

- **GEO-600** – A modified Michelson's interferometer. The differential strain is derived as a function of frequency to set bounds on the ALP couplings. The entire optimal frequency range of the detector (100 Hz -10 kHz) remains smaller than the fundamental frequency of the longitudinal oscillation mode  $\sim 37$  kHz. Sensitive to the ALP mass range  $m_a \approx 10^{-11} - 10^{-13}$  eV.
- **LIGO** – FC oscillations can also be probed with Fabry-Perot interferometers like LIGO. The methodology is similar to GEO600 but for LIGO the sensitivity is attenuated by a factor of arm cavity finesse  $\sim \mathcal{O}(100)$ . There is an additional contribution to  $\delta(L_x - L_y)$  from the thickness variation of the mirrors fitted on the two cavity arms. However, this is a subleading effect because  $\delta(L_x - L_y) \propto \Delta t \simeq \sim 80 \mu\text{m}$ . LIGO-03 observations set limits in the mass range  $m_a \approx 10^{-14} - 10^{-11}$  eV.

# Mechanical resonators



- Similar to optical cavities, mechanical resonators are sensitive to the time variation of the mechanical strain  $h(t)$  of solid objects consisting of many atoms, which originates in variations of the atom size caused by FC variations.

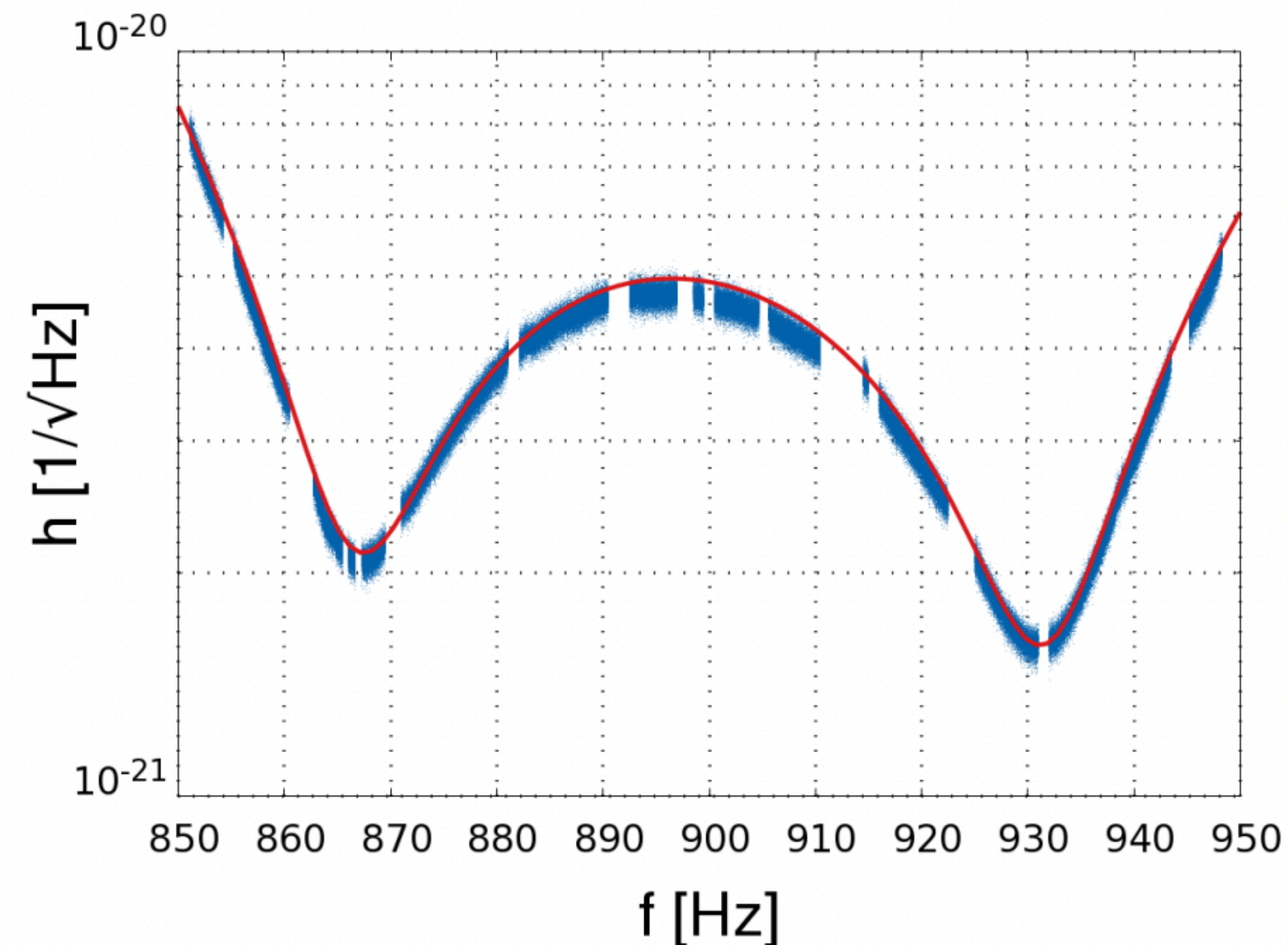
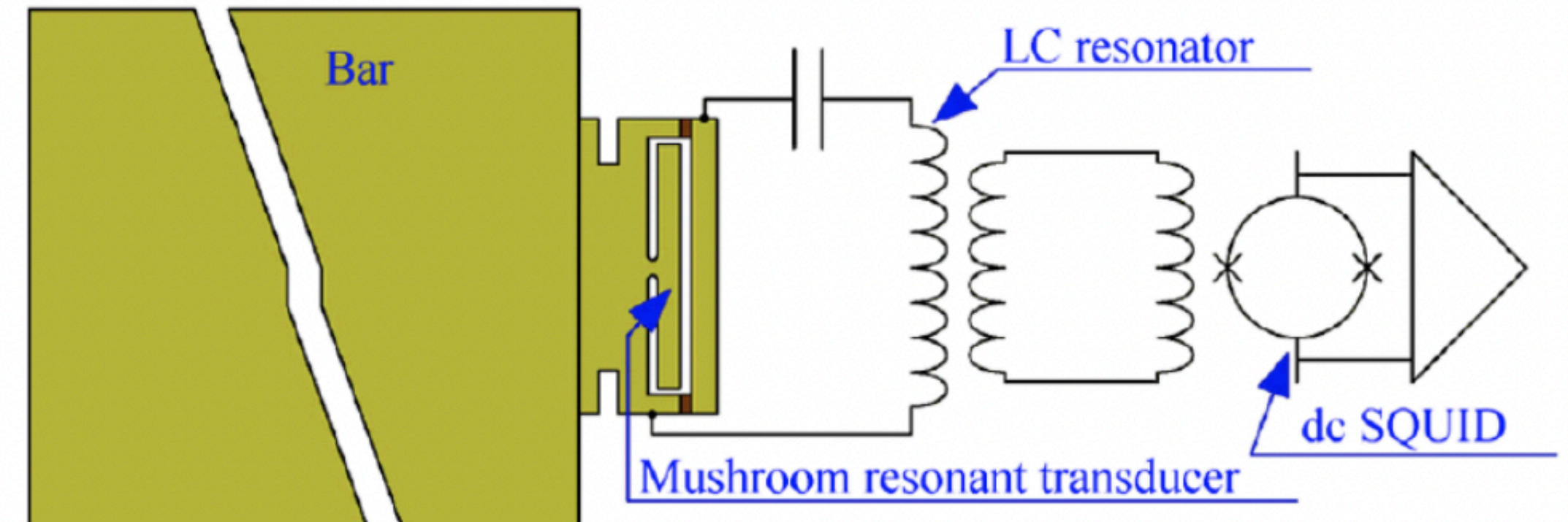
$$h(t) = -(\delta_\alpha(a) + \delta_e(a))$$

- For quadratic ALP couplings that induce the FC variations above, the strain can be resonantly enhanced if one of the acoustic modes of the elastic body is tuned to twice the ALP Compton frequency.

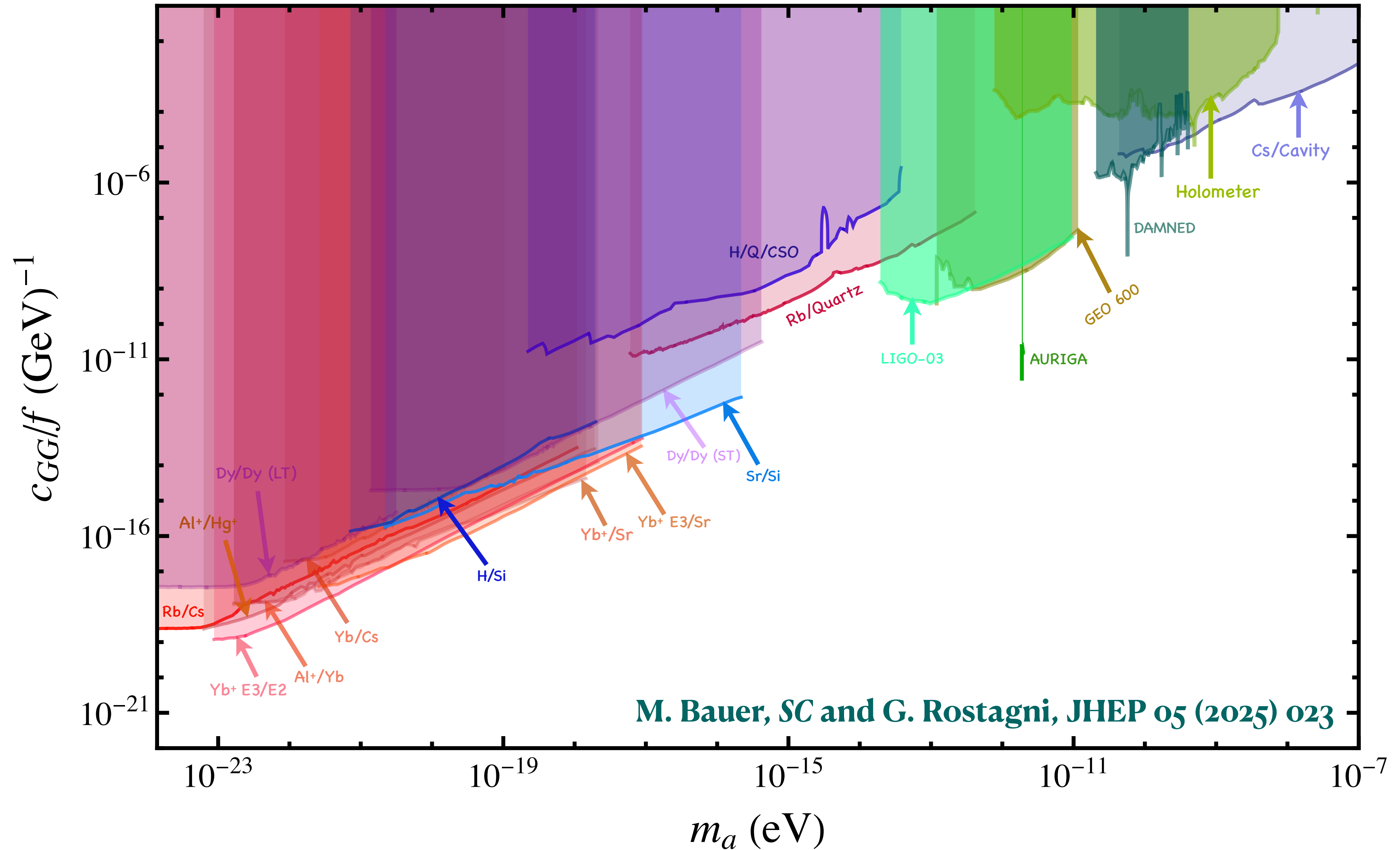


# Mechanical resonators

**AURIGA** – A cryogenic resonant-mass detector of bar length  $\sim \mathcal{O}(\text{m})$ .  
Sensitivity over a narrow bandwidth  
850-950 Hz, corresponding to ALP mass  
window 1.88 - 1.94 peV.



# Curtain call for current constraints



**The next-gen**



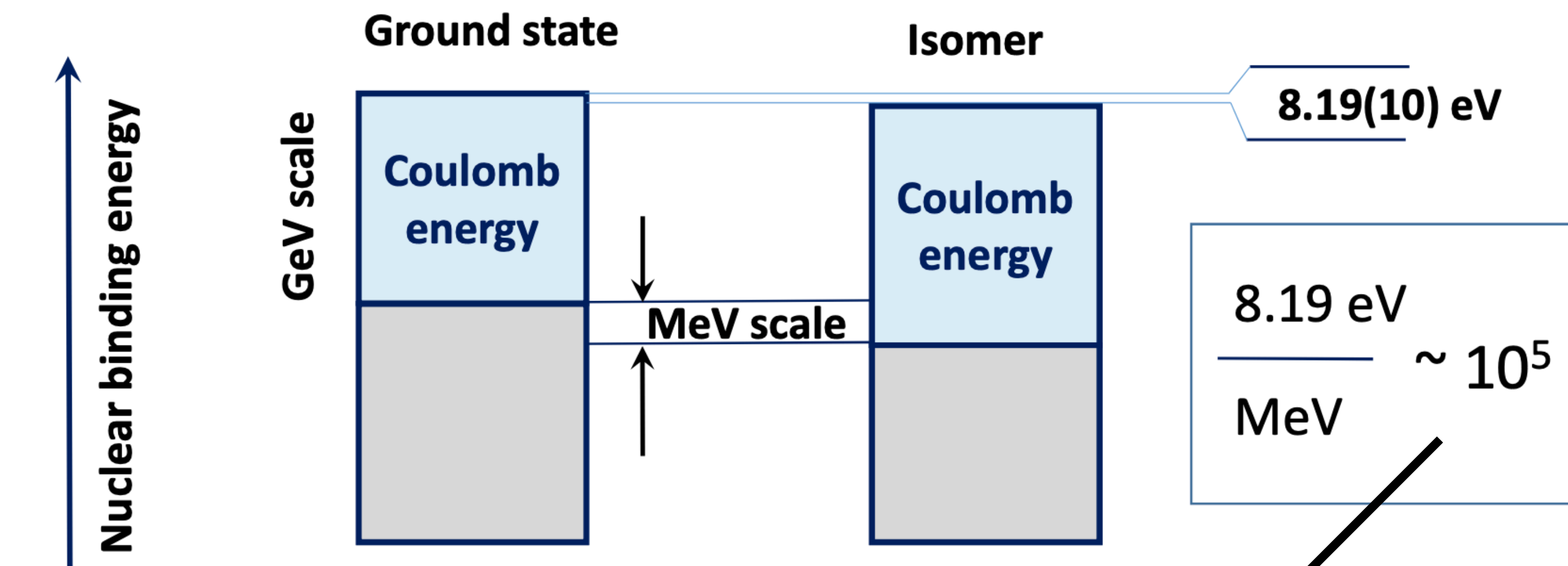
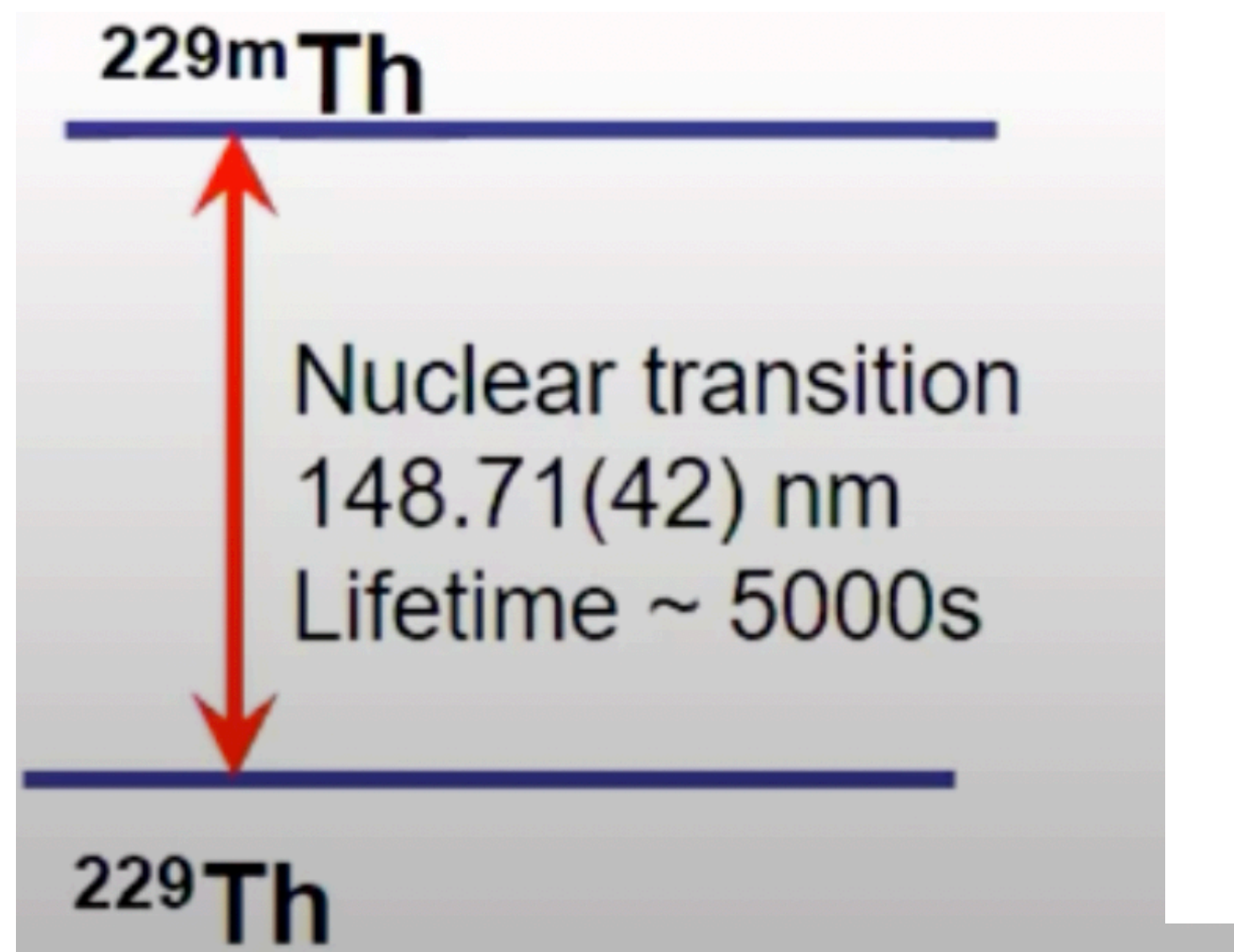
# Nuclear clock - $^{229}\text{Th}$

Seiferle et al., Nature 573, 243 (2019)

T. Sikorsky et al., Phys. Rev. Lett. 125, 142503 (2020)

Caputo et. al, arXiv 2407.17526

Th-229 has an exceptionally low-energy excited isomer state with an excitation energy of a few eV, making it the only nuclear transition accessible to lasers and precision spectroscopy.



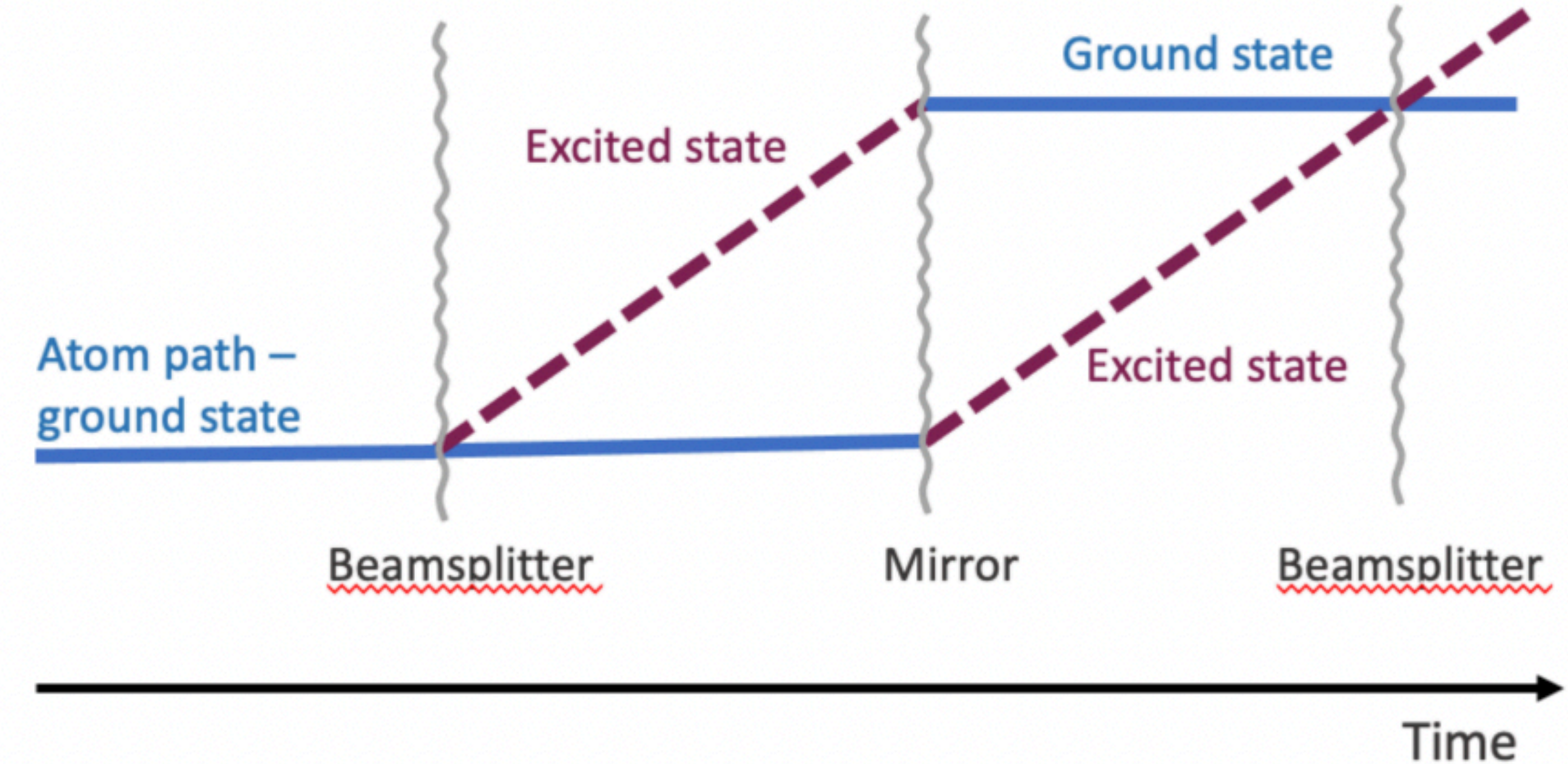
courtesy : M. Safronova

**Unprecedented sensitivity** - Corresponds to sensitivity coefficients  $k_\alpha, k_q \sim \mathcal{O}(10^4 - 10^5)$



# Atom interferometers

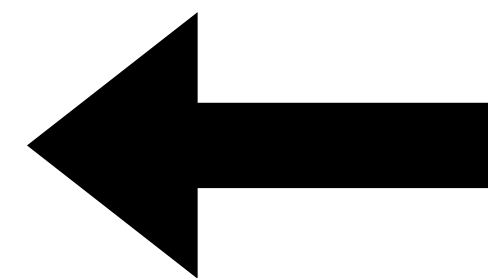
- Atomic interferometers measure the phase shift between split atomic wave packets and detect a dark matter-induced signal phase when the period of atomic transition oscillation matches the total duration of the interferometric sequence.
- The FC oscillations generate an oscillatory component in the electronic transition frequency, which is  $\omega_A \propto m_e \alpha^{2+\xi}$ .



$$\omega_A(t, x) = \omega_A + \delta\omega_A(a) \quad \frac{\delta\omega_A(a)}{\omega_A} = \delta_e(a) + (2 + \xi) \delta_\alpha(a)$$

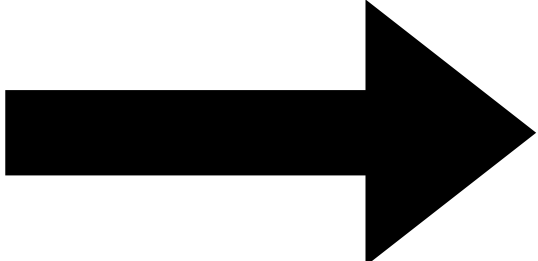
$$\approx (\delta_e + (2 + \xi)\delta_\alpha) \frac{\rho_{\text{DM}}}{m_a^2 f^2} \cos(2\omega_a t) \equiv \bar{\omega}_A \cos(2\omega_a t)$$

$$\Phi_{t_1}^{t_2} = \int_{t_1}^{t_2} \delta\omega_A(a) dt$$



The total phase difference for a single AI is obtained by summing over all such paths in which the atom is in the excited state

# Gradiometers



A system of two or more interferometers is used to cancel the common laser phase noise

separation between two AIs

$$\Phi_s = \frac{4 \bar{\omega}_A}{\omega_a} \frac{\Delta r}{L} \sin(\omega_a n L) \sin(\omega_a T) \sin\{\omega_a (T + (n-1)L)\}$$

Baseline length

Interrogation time

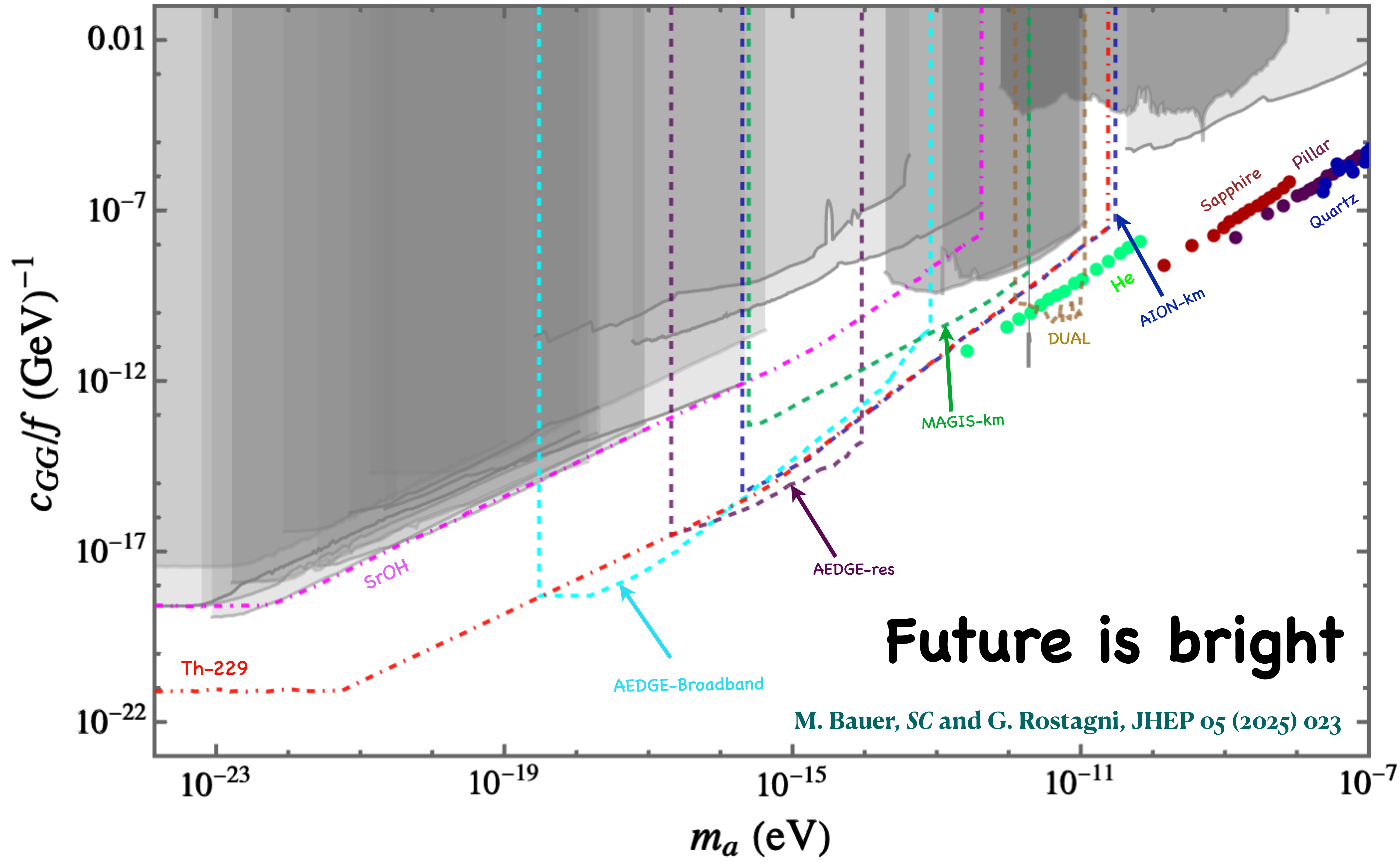
## Proposals

- Compact gradiometers : **AION-10** and **MAGIS**
- Longer baselines - 100 m and km length baselines
- Space based - **AEDGE**

$$\Phi_s = 4 \bar{\omega}_a n \Delta r \sin^2(m_a T)$$

- Longer baseline corresponds to higher sensitivity
- Low frequencies prone to gravity gradient noise





## Phenomenology Summary

- Oscillations in constants shift **atomic transition frequencies** and **cavity lengths**.
- Comparisons (clock–clock, clock–cavity, cavity–cavity) are sensitive to different combinations of  $\alpha, m_e, m_N$ .
- Experiments span broad mass ranges:
  - **Clocks** → probe the lowest frequencies (longest coherence times).
  - **Optical cavities** → extend to mid–frequency ranges.
  - **Interferometers** → sensitive at higher frequencies.
  - **Acoustic/mechanical resonators** → reach the highest mass windows.
- Current bounds already cover many orders of magnitude in parameter space.
- Future instrumentation promises **another 3–5 orders of magnitude gain in sensitivity**.

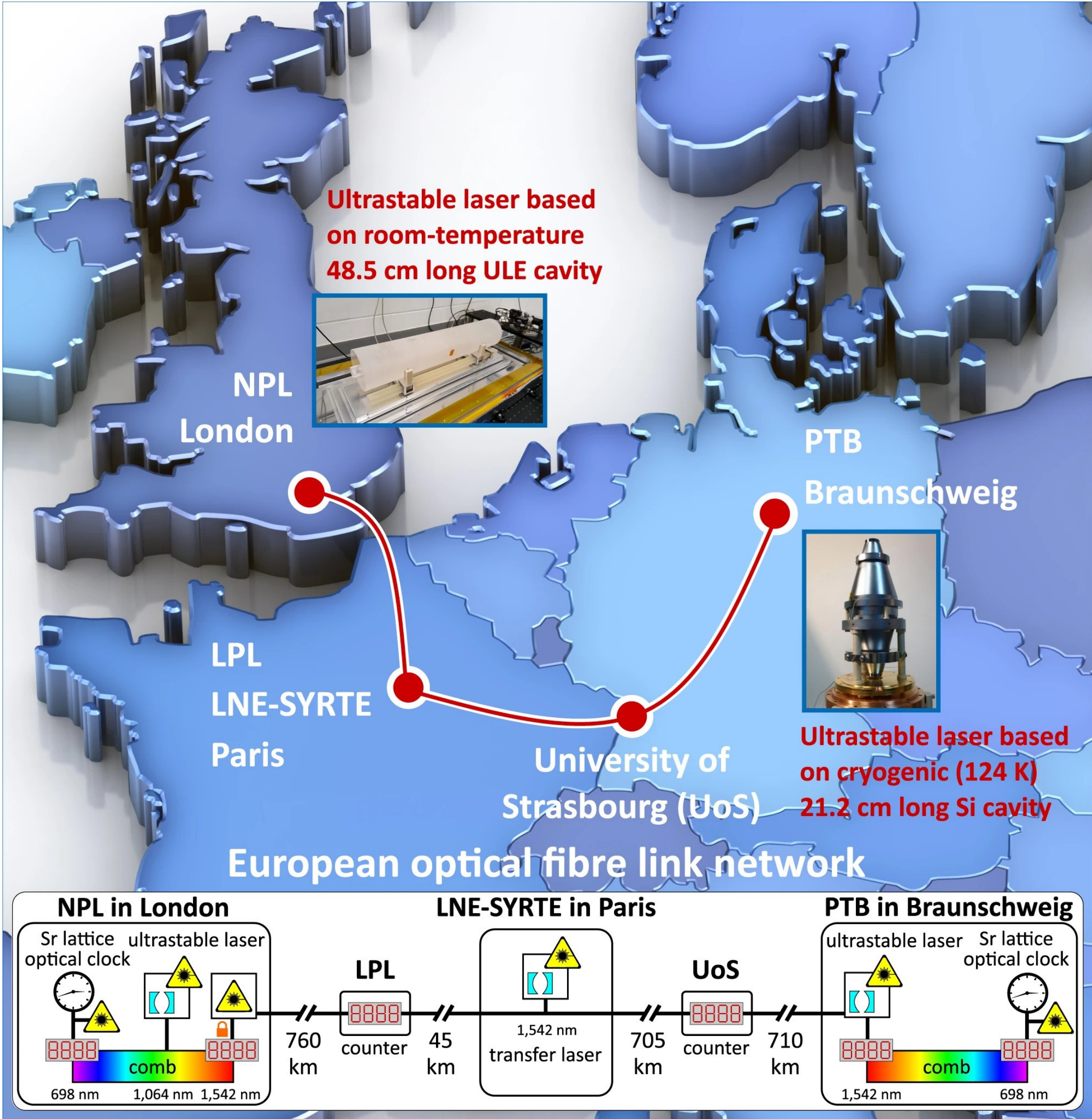
## Next Steps:

So we now know how oscillations show up in real instruments. The next step is to push beyond a single lab — and ask what happens when clocks and cavities are separated across large distances.

**Looking Ahead (with imagination)**



# Two clocks at a distance



ARTICLE

<https://doi.org/10.1038/s41467-021-27884-3>

OPEN

Check for updates

## Comparing ultrastable lasers at $7 \times 10^{-17}$ fractional frequency instability through a 2220 km optical fibre network

M. Schioppo<sup>1,7</sup>, J. Kronjäger<sup>1,7</sup>, A. Silva<sup>1</sup>, R. Ilieva<sup>1</sup>, J. W. Paterson<sup>1</sup>, C. F. A. Baynham<sup>1</sup>, W. Bowden<sup>1</sup>, I. R. Hill<sup>1</sup>, R. Hobson<sup>1</sup>, A. Vianello<sup>1</sup>, M. Dovale-Álvarez<sup>1</sup>, R. A. Williams<sup>1</sup>, G. Marra<sup>1</sup>, H. S. Margolis<sup>1</sup>, A. Amy-Klein<sup>2</sup>, O. Lopez<sup>2</sup>, E. Cantin<sup>2,3</sup>, H. Álvarez-Martínez<sup>3,4</sup>, R. Le Targat<sup>3</sup>, P. E. Pottie<sup>3</sup>, N. Quintin<sup>5</sup>, T. Legero<sup>6</sup>, S. Häfner<sup>6</sup>, U. Sterr<sup>6</sup>, R. Schwarz<sup>6</sup>, S. Dörscher<sup>6</sup>, C. Lisdat<sup>6</sup>, S. Koke<sup>6</sup>, A. Kuhl<sup>6</sup>, T. Waterholter<sup>6</sup>, E. Benkler<sup>6</sup> & G. Grosche<sup>6</sup>

Ultrastable lasers are essential tools in optical frequency metrology enabling unprecedented measurement precision that impacts on fields such as atomic timekeeping, tests of funda-

PHYSICAL REVIEW LETTERS 134, 031001 (2025)

### Ultralight Dark Matter Search with Space-Time Separated Atomic Clocks and Cavities

Melina Filzinger<sup>1,\*</sup>, Ashlee R. Caddell<sup>2,\*</sup>, Dhruv Jani<sup>2</sup>, Martin Steinle<sup>1</sup>, Leonardo Giani<sup>2</sup>, Nils Huntemann<sup>1</sup> and Benjamin M. Roberts<sup>2,†</sup>

<sup>1</sup>Physikalisch-Technische Bundesanstalt, Bundesallee 100, 38116 Braunschweig, Germany

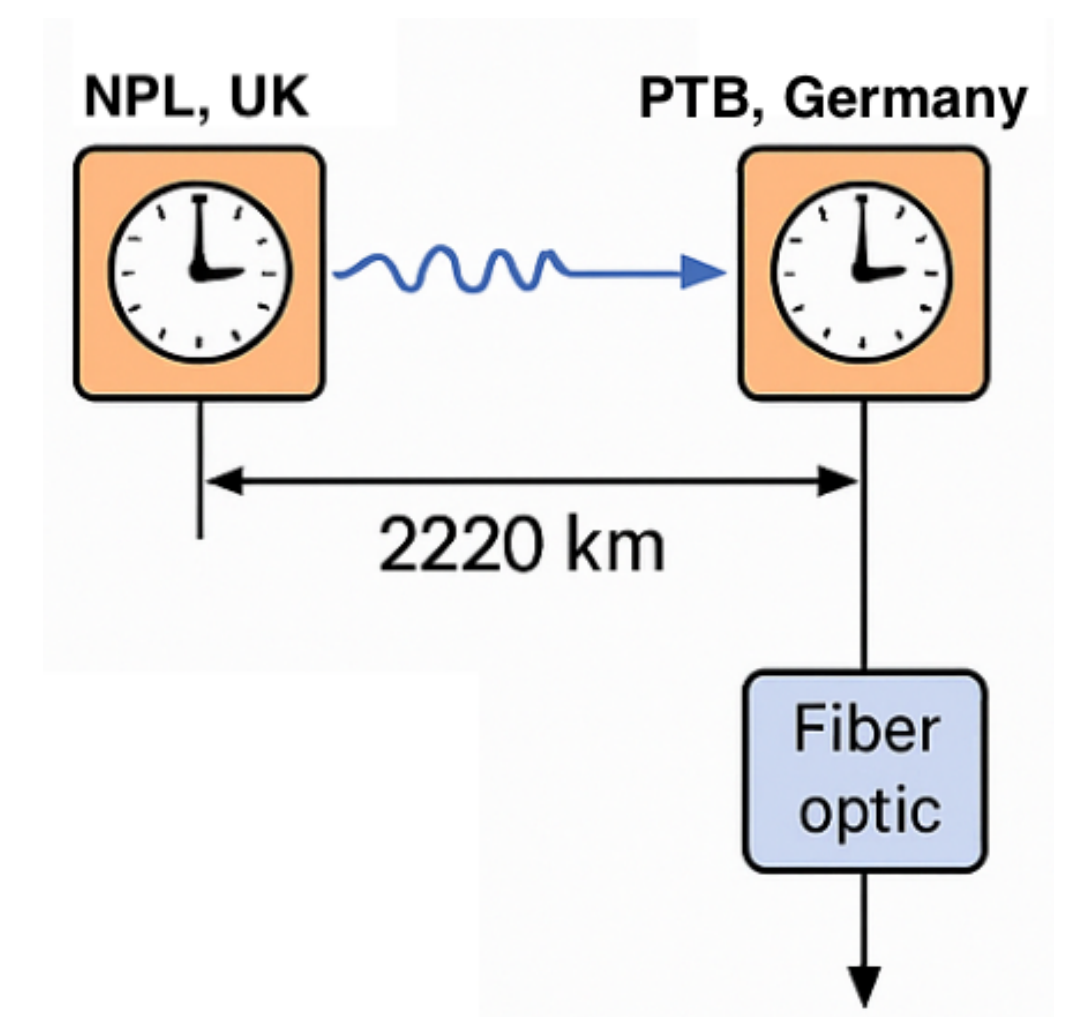
<sup>2</sup>School of Mathematics and Physics, The University of Queensland, Brisbane, Queensland 4072, Australia

(Received 21 December 2023; revised 17 September 2024; accepted 18 December 2024; published 23 January 2025)



# Two clocks at a distance

- Time delay through the fibre cancels out any time-dependent oscillation both clocks see, including part of the signal!
- But the spatial phase difference survives.



$$\delta\phi(t) \propto \phi(\vec{x}_B, t) - \phi(\vec{x}_A, t)$$

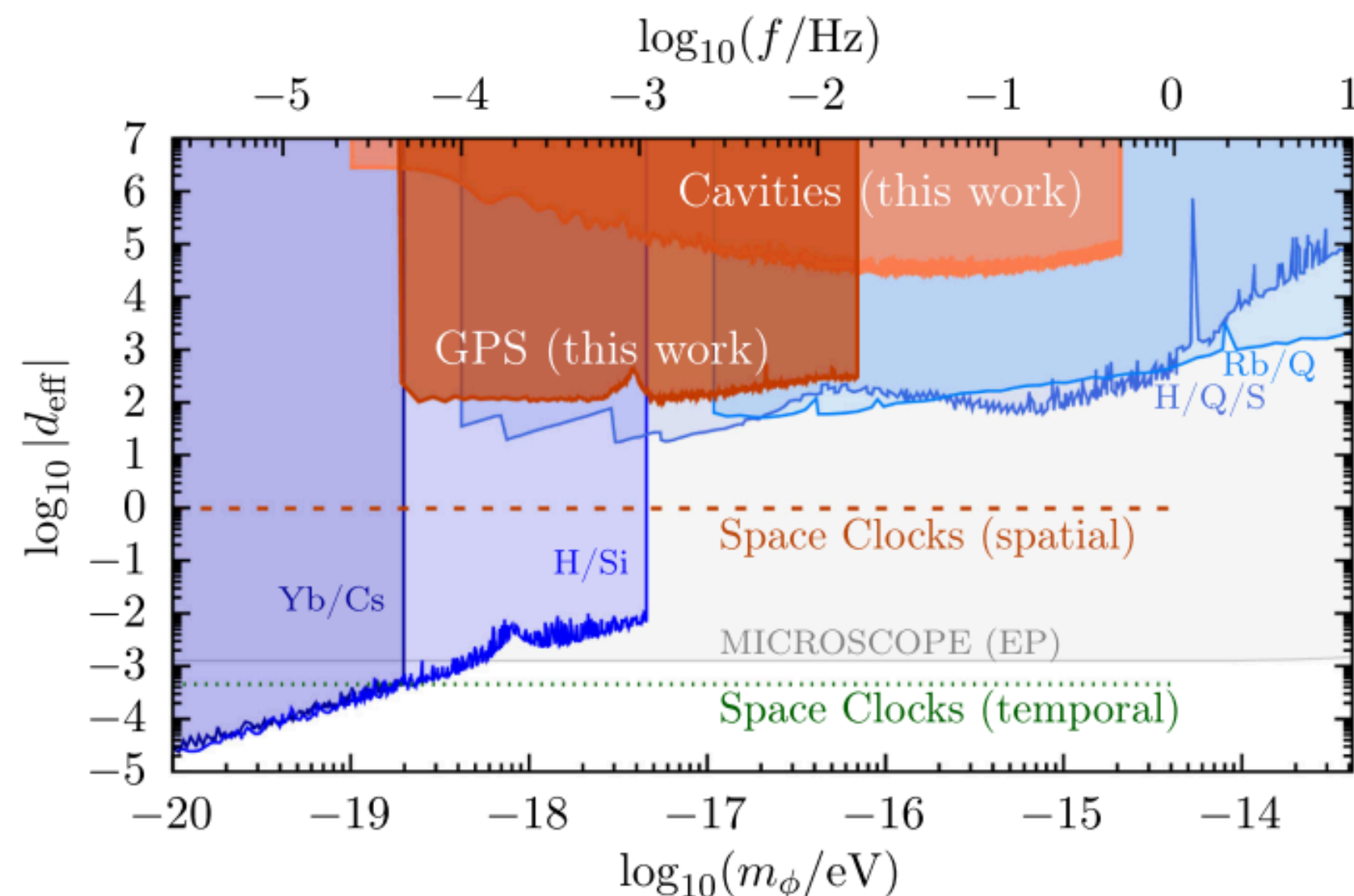
$$\Rightarrow \delta\phi(t) \propto \cos(m_\phi t - \vec{k} \cdot \vec{x}_B) - \cos(m_\phi t - \vec{k} \cdot \vec{x}_A)$$

$$\phi(t, \mathbf{x}) = \phi_0 \cos(\omega t - \mathbf{k} \cdot \mathbf{x}), \quad \omega \approx m_\phi, \phi_0 = \frac{\sqrt{2\rho_{\text{DM}}}}{m_\phi}$$

$$k = m_\phi v, v \sim 10^{-3}$$

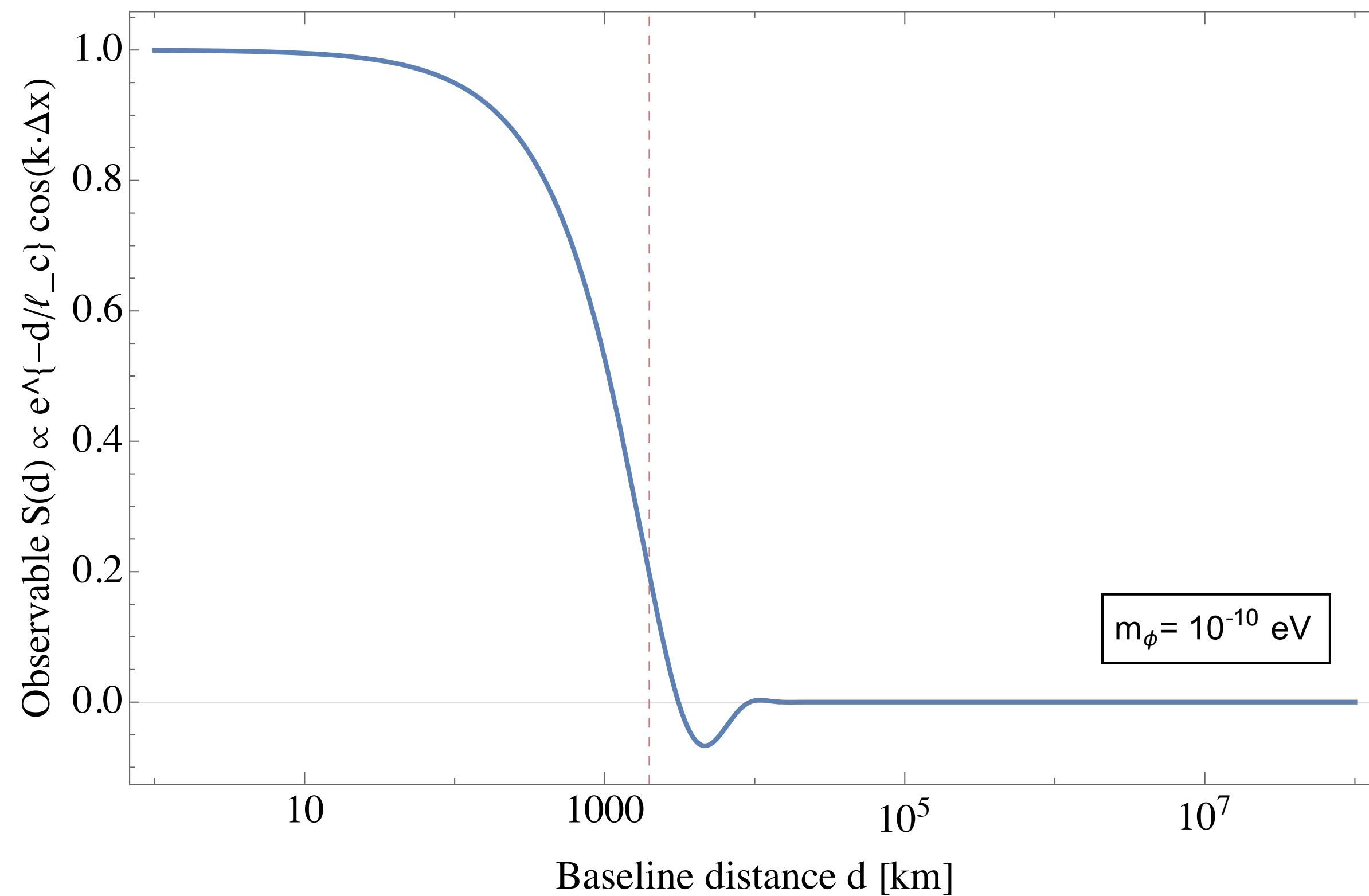
$$\frac{\delta(\nu^A/\nu^B)}{\nu^A/\nu^B} = \kappa\phi_0(d_{m_e} + d_e) \frac{\omega D \mathbf{n} \cdot \mathbf{v}}{c^2} \sin(\omega t).$$

signal proportional to baseline



# Longer baseline=stronger signal??

Signal grows with  $D$  until  $D \sim l_c \simeq 2\pi/(m_\phi v_0)$ , beyond that it decorrelates.

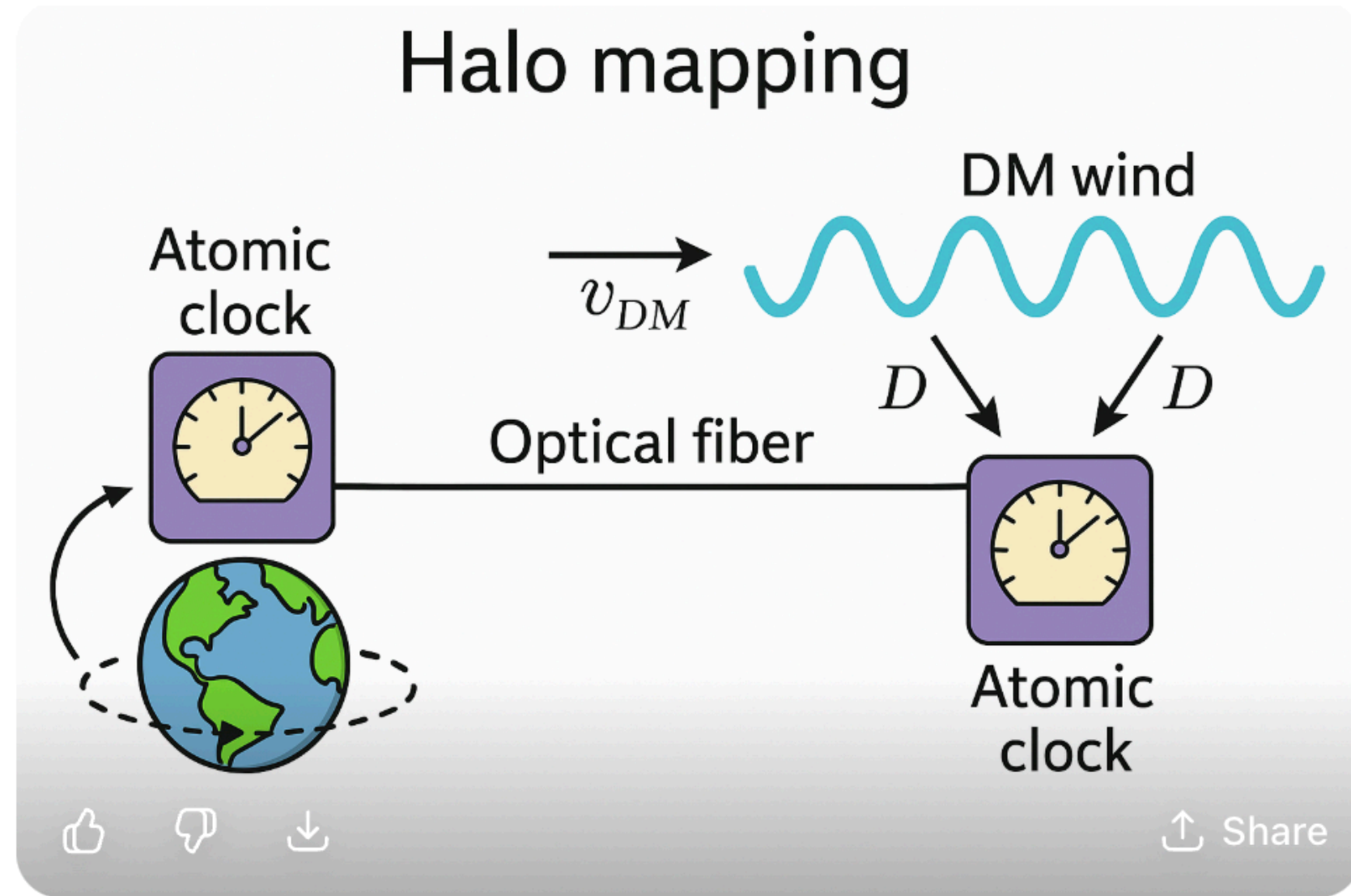


$$\frac{\delta(\nu^A/\nu^B)}{\nu^A/\nu^B} \propto \kappa \phi_0 \frac{\omega}{c^2} e^{-D^2/(2\ell_c^2)}$$

$$D \ll l_c$$



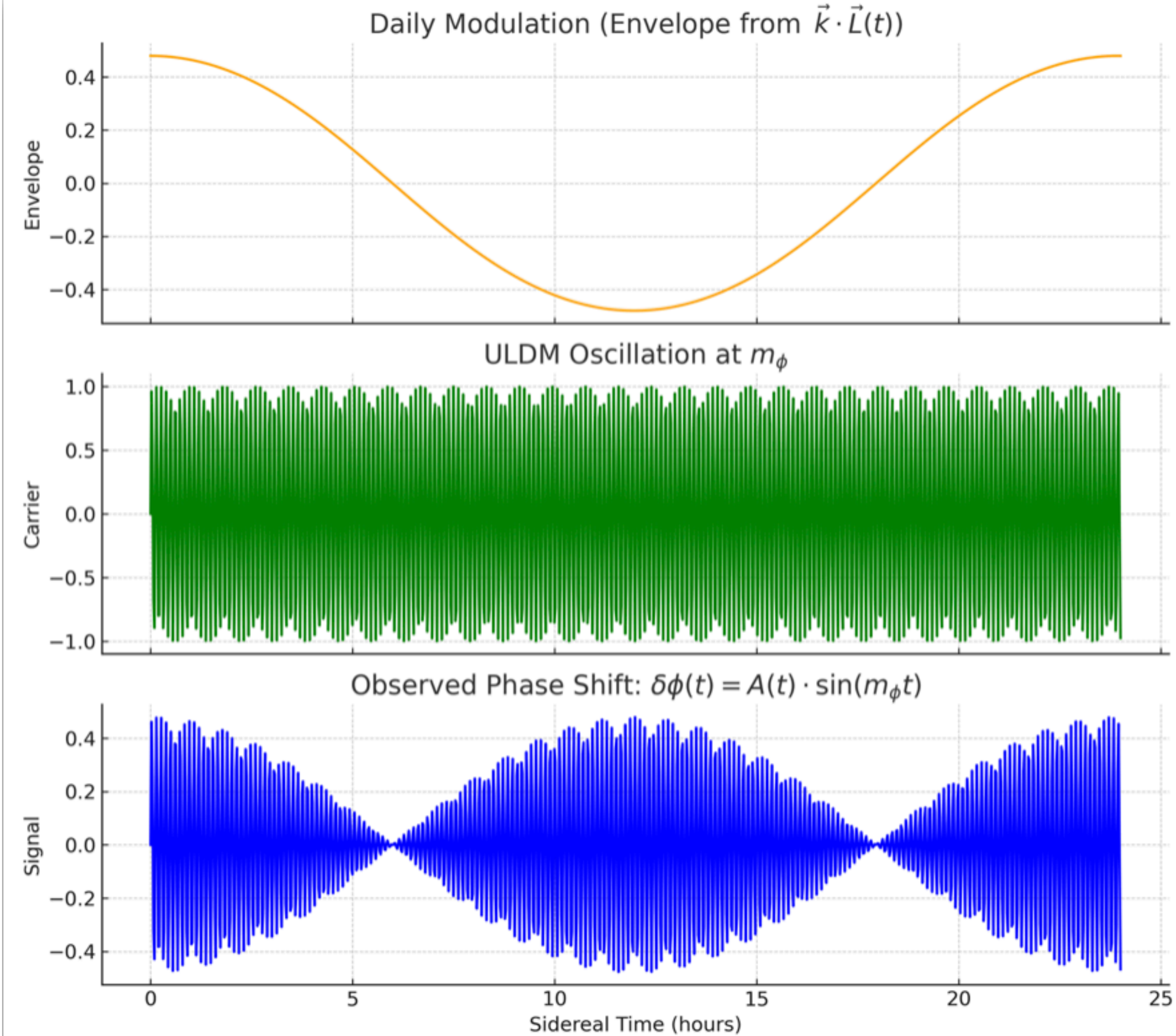
# Dark matter wind



$$\delta\phi(t) = A \cdot \sin\left(\frac{\vec{k} \cdot \vec{L}}{2}\right) \cdot \sin\left(m_\phi t - \vec{k} \cdot \vec{x}_{\text{mid}}\right)$$

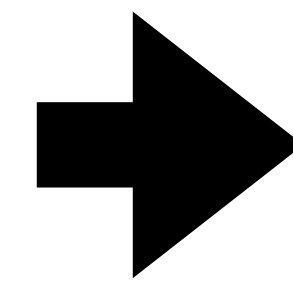
The **amplitude** of the signal modulates with  $\vec{v}_{DM} \cdot \vec{L} \rightarrow$  gives **sidereal signal**.

The **frequency** is set by the ULDM mass  $m_\phi$ .





Place one clock at each fibre node



**Wind mapping?**

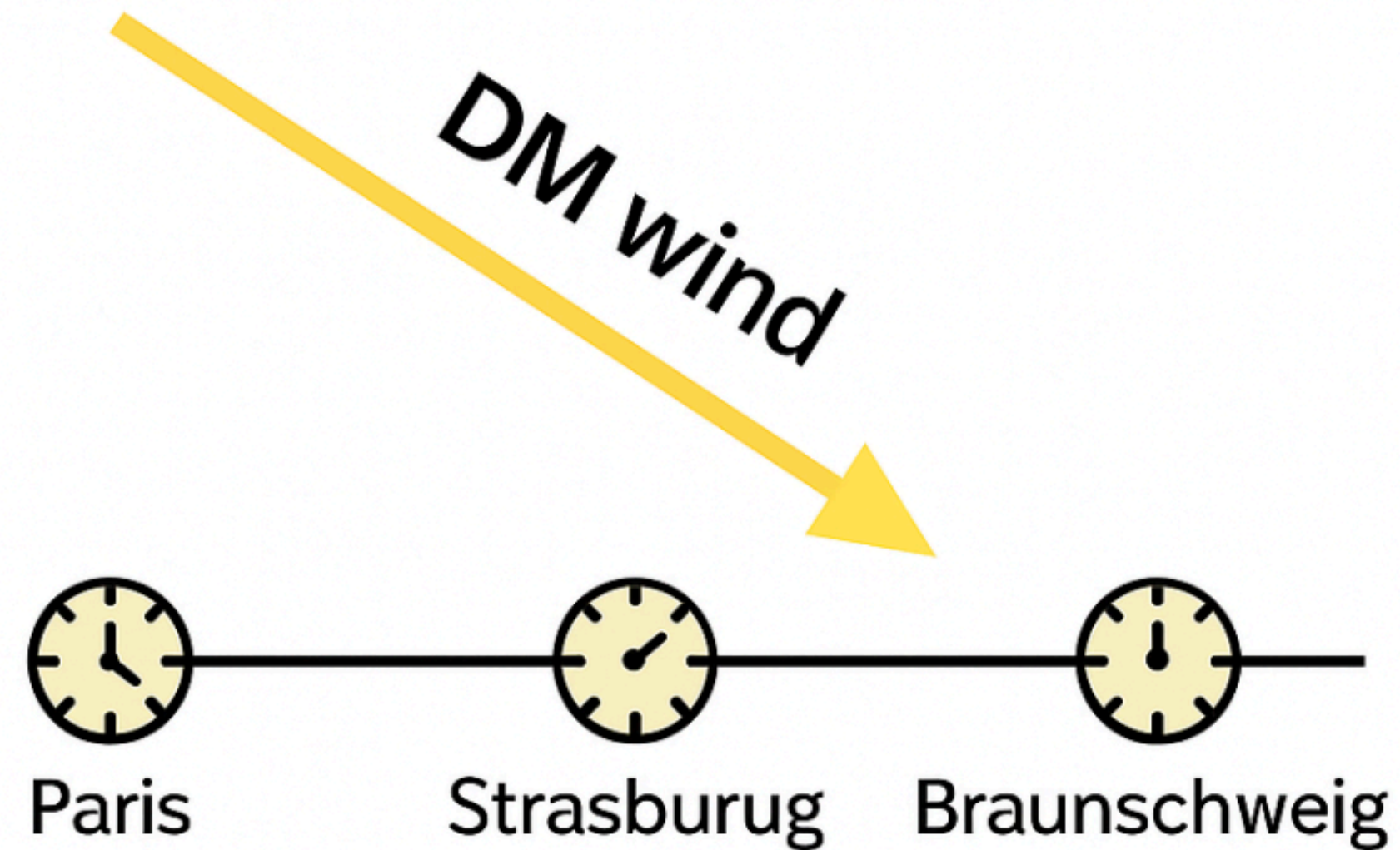
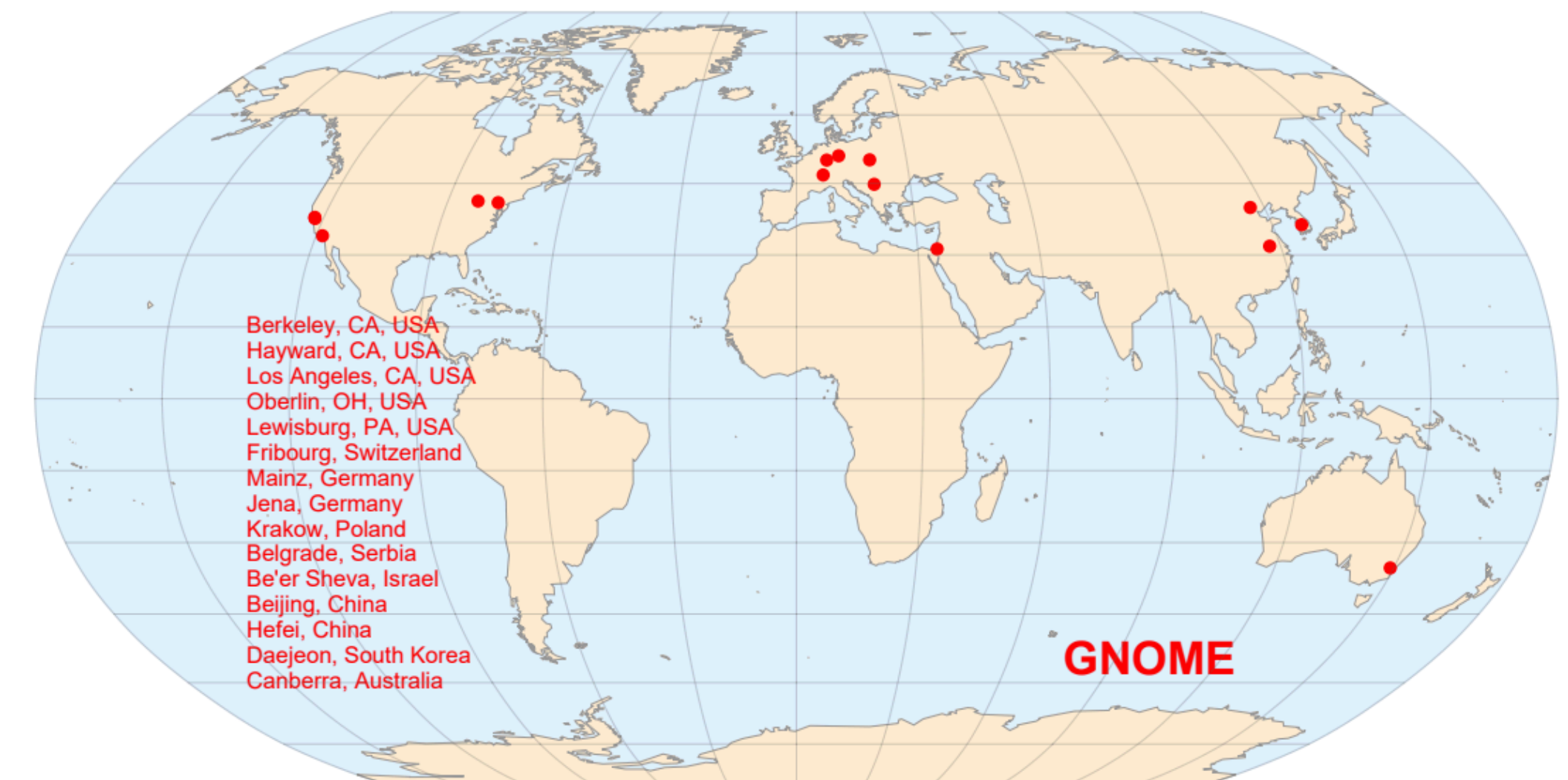
Annalen der Physik / Volume 536, Issue 1 / 2300083

Review | [Full Access](#)

**What Can a GNOME Do? Search Targets for the Global Network of Optical Magnetometers for Exotic Physics Searches**

[Correction\(s\) for this article >](#)

Samer Afach, Deniz Aybas Tumturk, Hendrik Bekker, Ben C. Buchler, Dmitry Budker, Kaleb Cervantes, Andrei Derevianko, Joshua Eby, Nataniel L. Figueroa, Ron Folman ... [See all authors](#) ▾



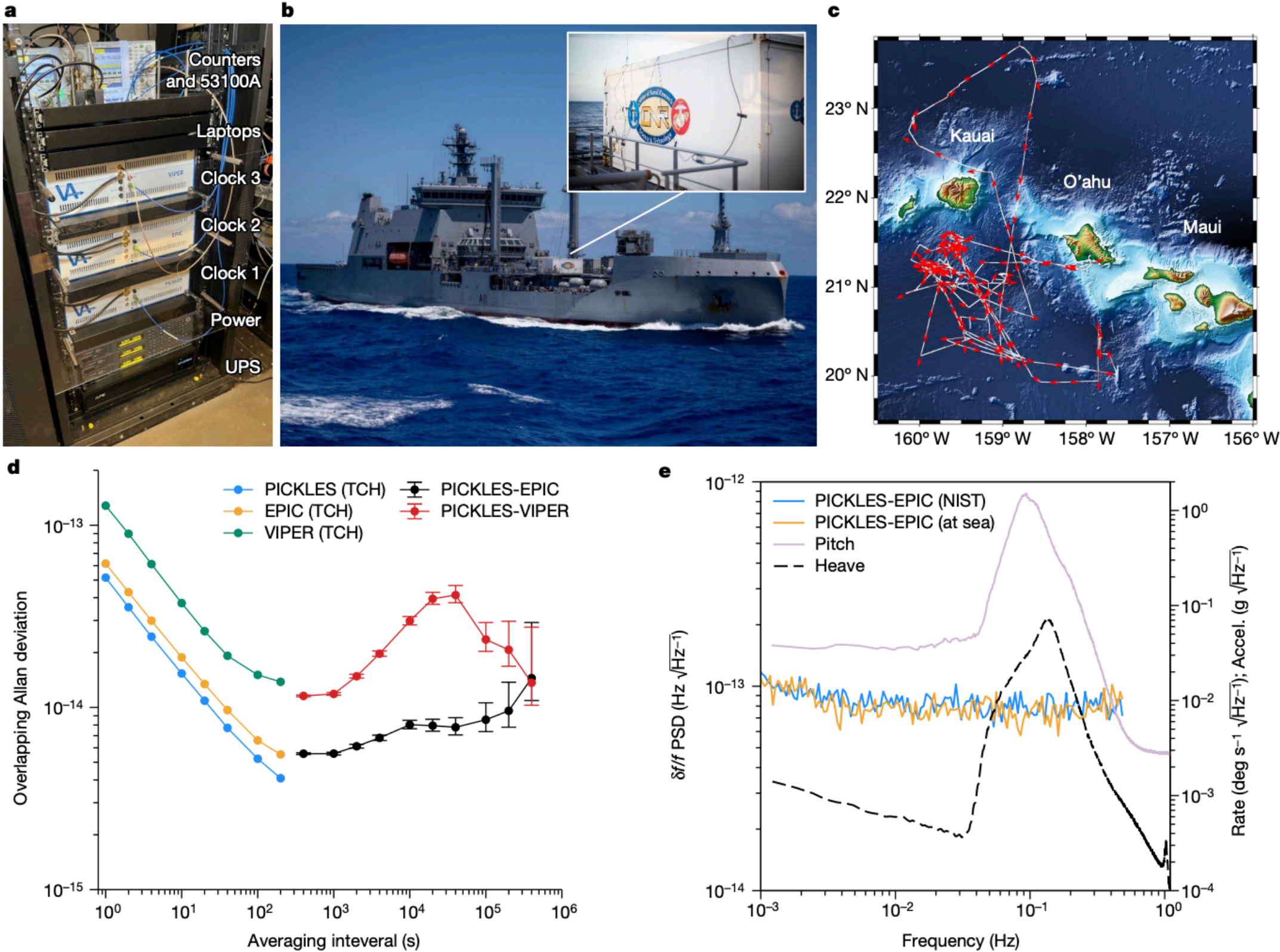
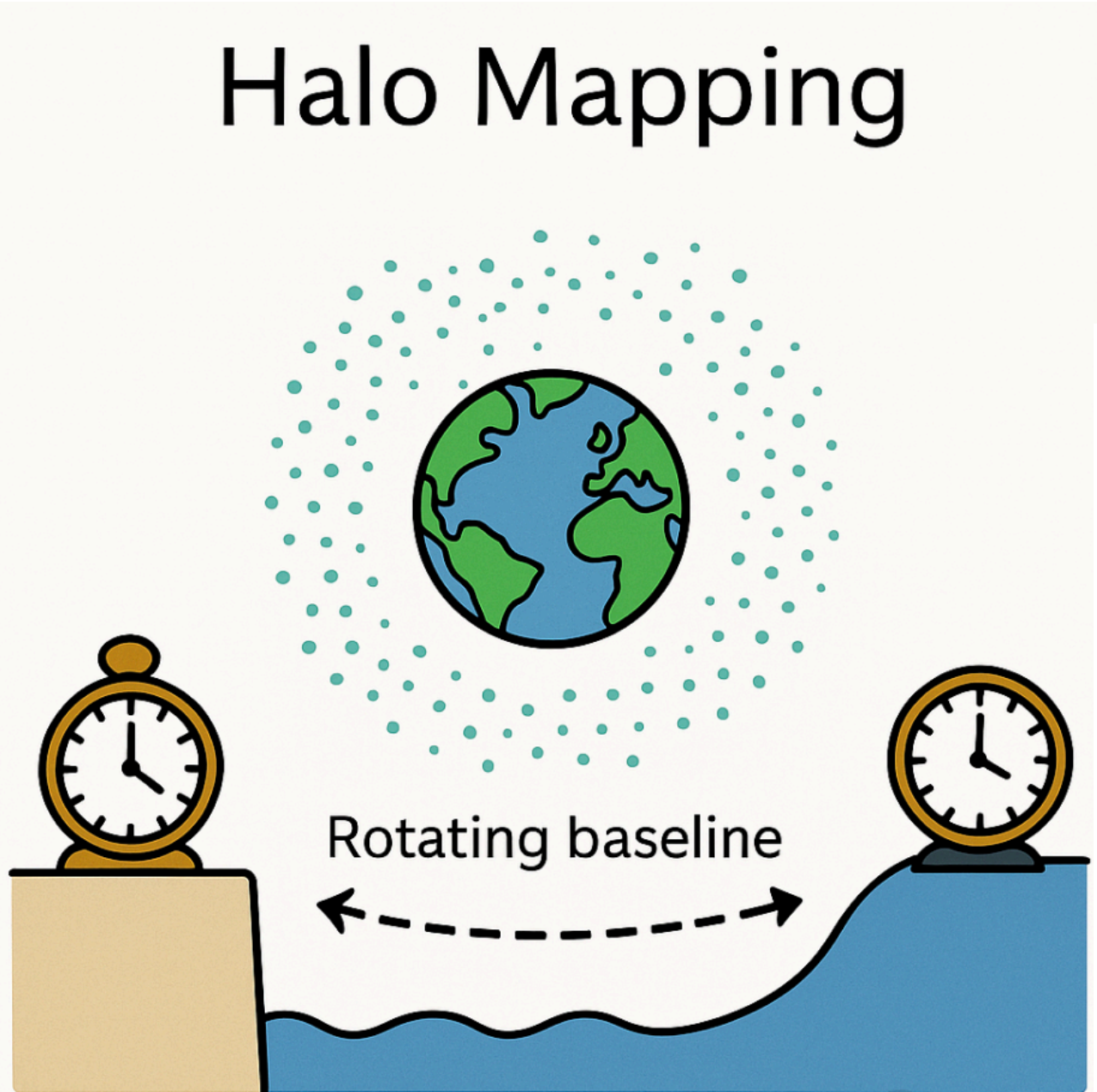
$$\delta\phi_i(t) \propto \sin\left(\frac{k \cdot D_i}{2}\right)$$

Each baseline  $D_i \rightarrow$  different projection  $k \cdot D_i$

Combine  $\rightarrow$  average over DM velocity distribution  $\rightarrow$  wind direction ( $\approx$  2D halo mapping)



# One at sea (!) and one on shore?



**nature**

Explore content ▾About the journal ▾Publish with us ▾

[nature](#) > [articles](#) > [article](#)

Article | [Open access](#) | Published: 24 April 2024

**Optical clocks at sea**

[athan D. Roslund](#) , [Arman Cingöz](#), [William D. Lunden](#), [Guthrie B. Partridge](#), [Abijith S. Kowligy](#), [Franker](#), [Daniel B. Sheredy](#), [Gunnar E. Skulason](#), [Joe P. Song](#), [Jamil R. Abo-Shaer](#) & [Martin M. Boyd](#)

[ure](#) 628, 736–740 (2024) | [Cite this article](#)

Accesses | 46 Citations | 140 Altmetric | [Metrics](#)

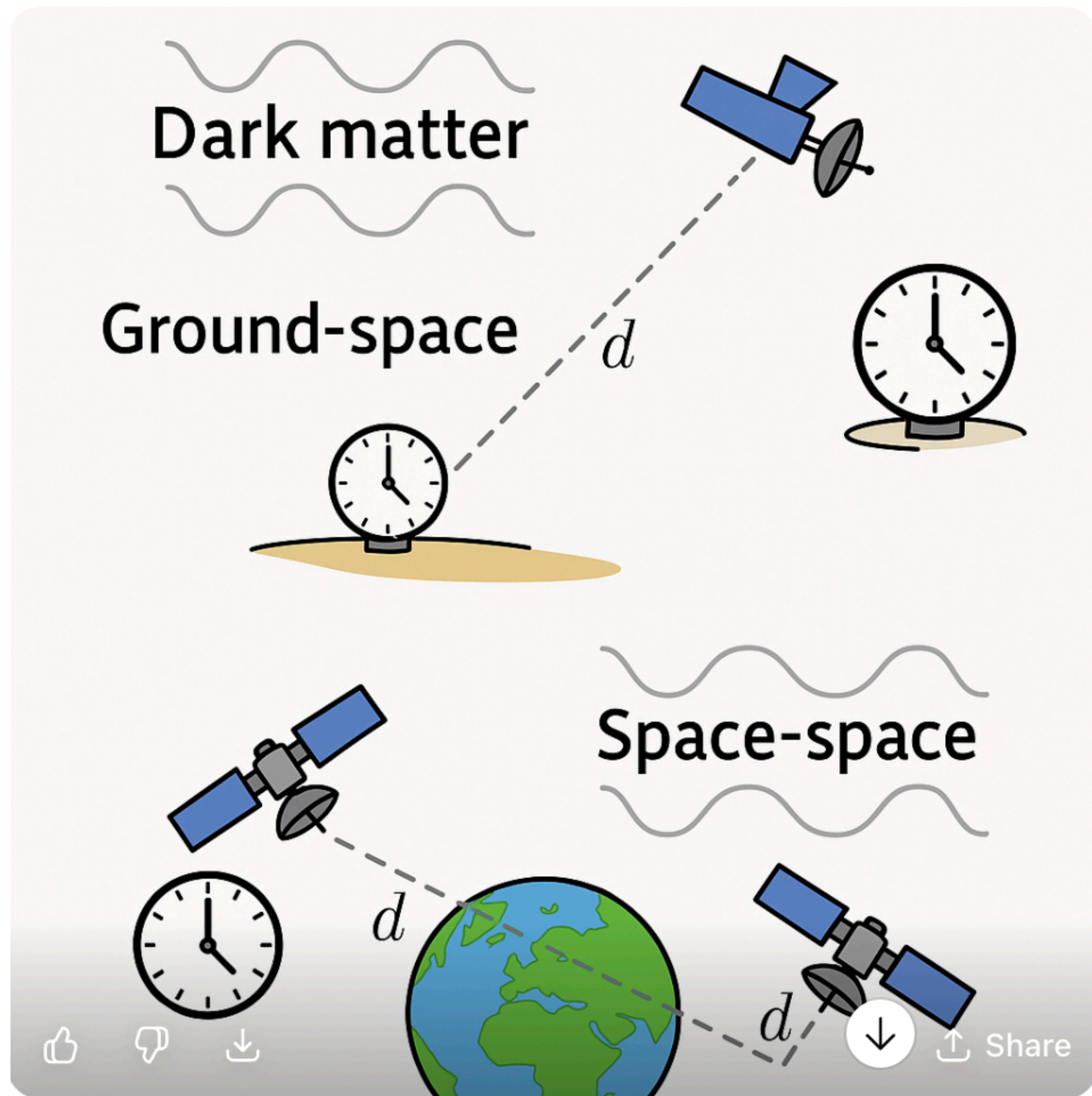
**Abstract**

Deployed optical clocks will improve positioning for navigational autonomy<sup>1</sup>, provide remote

Rotating baseline : ideal for wind mapping if the systematics can be handled!!



# What else?



- Possible 3D halo mapping potential
- Different systematics in space
- Expensive technology

## Final Summary

Ultralight dark matter offers a wave-like alternative to WIMPs, accessible through the extraordinary precision of quantum technologies — clocks, interferometers, and resonators.

For axions and ALPs, it's mainly the quadratic, scalar-like couplings that these machines probe. Though suppressed at high scales, they fall squarely within reach of today's sensors.

Looking ahead, longer integration times, improved stabilities, and eventually global networks of quantum sensors promise leaps in sensitivity. It's a young but very promising field — one that's clearly worth the investment.



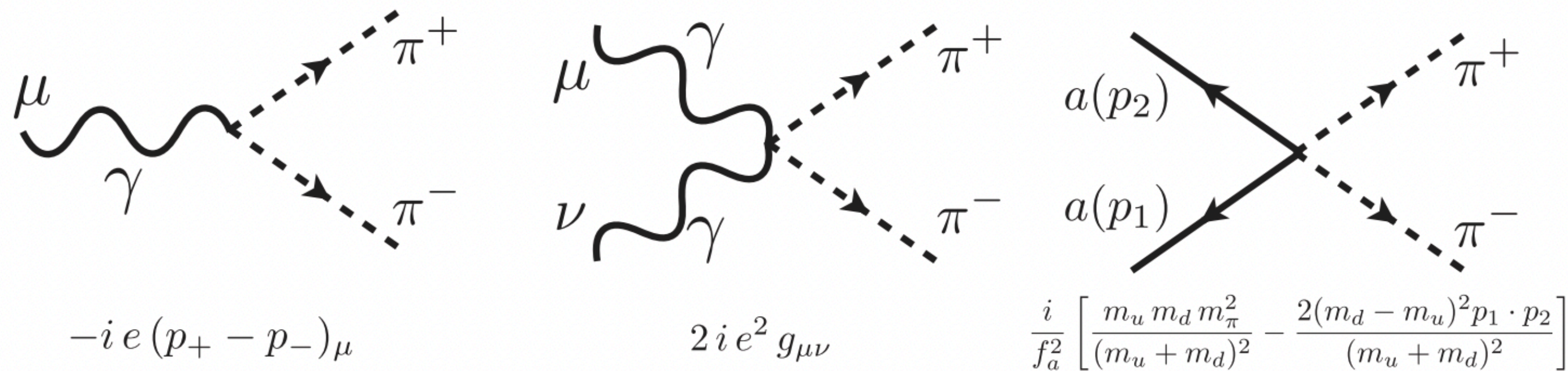
**Thank you!!**

# Pions

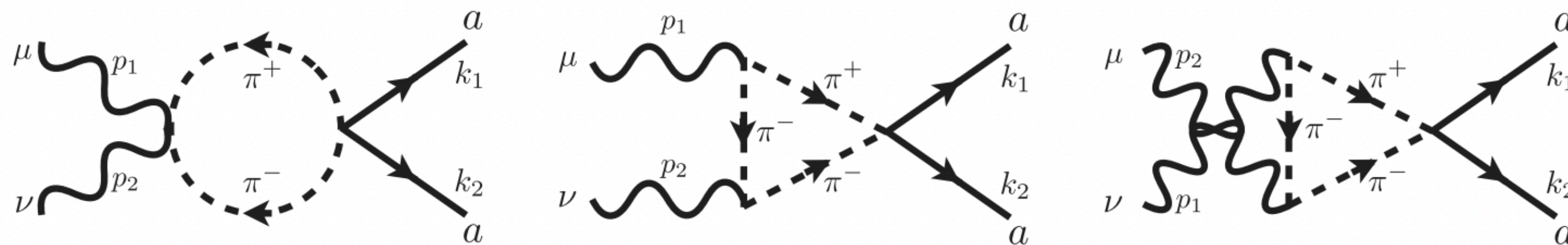
$$\mathcal{L}_{\chi\text{PT}} = \frac{f_\pi^2}{4} \text{tr}[\Sigma m_q(a)^\dagger + m_q(a) \Sigma^\dagger] + \dots,$$

where  $\Sigma = \exp(i\sqrt{2}\Pi/f_\pi)$  and the quark mass matrix is ALP-field dependent

$$m_q(a) = e^{-i\kappa_q \frac{a}{f} c_{GG}} m_q e^{-i\kappa_q \frac{a}{f} c_{GG}},$$



Feynman rules for the vertices from the  $\mathcal{O}(p^2)$  chiral Lagrangian leading to a loop-induced  $a^2 F^2$  coupling.



Three diagrams contributing to  $\gamma\gamma \rightarrow aa$  at  $\mathcal{O}(p^4)$  in the  $\chi\text{PT}$  Lagrangian.



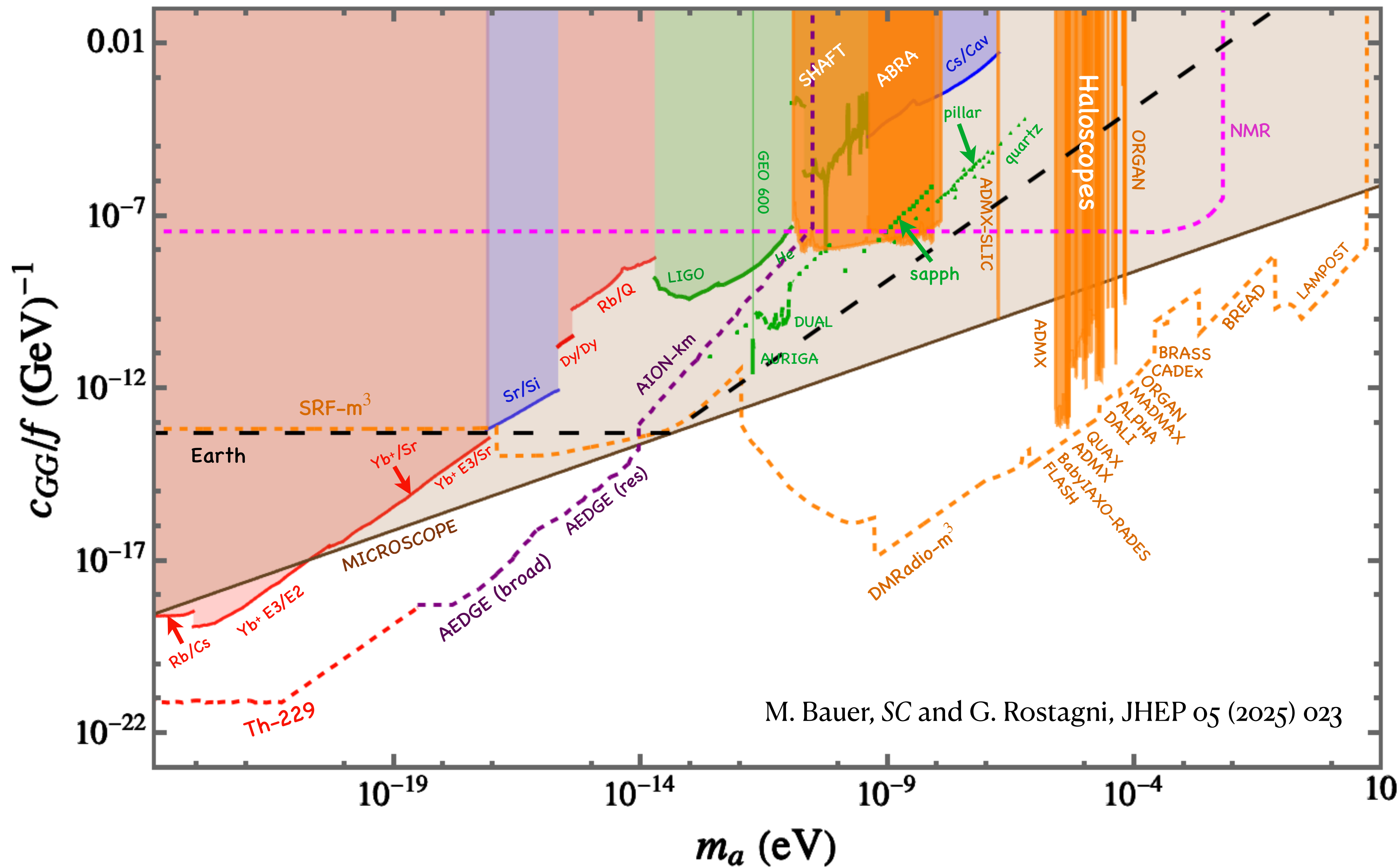
# Nucleons

$$\mathcal{L}_{\chi\text{PT}}^{(2)} = c_1 \text{tr}[\chi_+] \bar{N} N + \dots ,$$

$$\chi_+ = 2B_0 (\xi^\dagger m_q(a) \xi^\dagger + \xi m_q^\dagger(a) \xi)$$

$$M_N = M_0 - 4c_1 m_\pi^2$$

$$c_1 \text{tr}[\chi_+] \bar{N} N = C_N \frac{a^2}{f^2} \bar{N} N + \dots = 4c_1 m_\pi^2 \delta_\pi(a) \bar{N} N + \dots$$



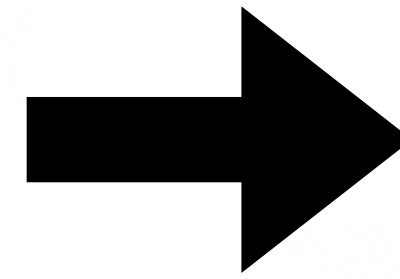


# Finite density effects

Axion-field value is different in the vicinity of a massive object (such as the earth) than in the vacuum.

$$(\partial_t^2 - \Delta + m_a^2)a = -\sin\left(\frac{a}{f}\right) \sum_i \frac{Q_i^{\text{source}} \delta_i}{f} \rho_{\text{source}}(r)$$

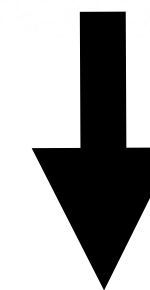
$$= -\frac{a}{f} \sum_i \frac{Q_i^{\text{source}} \delta_i}{f} \rho_{\text{source}}(r) + \mathcal{O}\left(\frac{a^3}{f^3}\right)$$



The source term up to quadratic axion interactions can be absorbed in the effective mass term

$$\bar{m}_a^2(r) = m_a^2 + \sum_i \frac{Q_i^{\text{source}} \delta_i}{f^2} \rho_{\text{source}}(r)$$

$$(\partial_t^2 - \Delta + \bar{m}_a^2(r))a = 0.$$



$$a(t, r) = \frac{\sqrt{2\rho_{\text{DM}}}}{m_a} \cos(m_a t) \left[ 1 - Z_\delta J_\pm(\sqrt{3|Z_\delta|}) \frac{R_{\text{source}}}{r} \right]$$

axion field at infinity takes the oscillating galactic background field

$$a(t, r) = \frac{\sqrt{2\rho_{\text{DM}}}}{m_a} \cos(m_a t) \left[ 1 - Z_\delta J_\pm(\sqrt{3|Z_\delta|}) \frac{R_{\text{source}}}{r} \right]$$

$$Z_\delta = \frac{1}{4\pi f^2} \frac{M_{\text{source}}}{R_{\text{source}}} \sum_i Q_i^{\text{source}} \delta_i$$

$$J_+(x) = \frac{3}{x^3} (x - \tanh x),$$

$$J_-(x) = \frac{3}{x^3} (\tan x - x).$$

$Q_i$ 's are positive,  $\delta_i$ 's are negative

$J_-(x)$  diverges for  $x \rightarrow \pi/2$

$$\frac{c_{GG}}{f} \gtrsim \left( \frac{6}{\pi^3} \frac{m_u m_d}{(m_u + m_d)^2} \frac{M_\oplus}{R_\oplus} |Q_{\hat{m}}| \right)^{-1/2} \approx \frac{1}{10^{15}} \text{ GeV}^{-1}$$

$$Q_{\hat{m}} = \left[ 9.3 - \frac{3.6}{A^{1/3}} - 2 \frac{(A-2Z)^2}{A^2} - 0.014 \frac{Z(Z-1)}{A^{4/3}} \right] \times 10^{-2},$$

$$Q_{\Delta M} = 1.7 \times 10^{-3} \frac{A-2Z}{A},$$

$$Q_\alpha = \left[ -1.4 + 8.2 \frac{Z}{A} + 7.7 \frac{Z(Z-1)}{A^{4/3}} \right] \times 10^{-4},$$

$$Q_e = 5.5 \times 10^{-4} \frac{Z}{A},$$

*Damour, Donoghue, et. al*

$$\delta_\pi = -2c_{GG}^2 \frac{m_u m_d}{(m_u + m_d)^2}$$

$$\delta_N = -4c_1 \frac{m_\pi^2}{M_N} \delta_\pi,$$

$$\delta_{\Delta M} = \delta_\pi,$$

$$\delta_\alpha = \frac{1}{12\pi} \left( 1 - 32c_1 \frac{m_\pi^2}{M_N} \right) \delta_\pi,$$

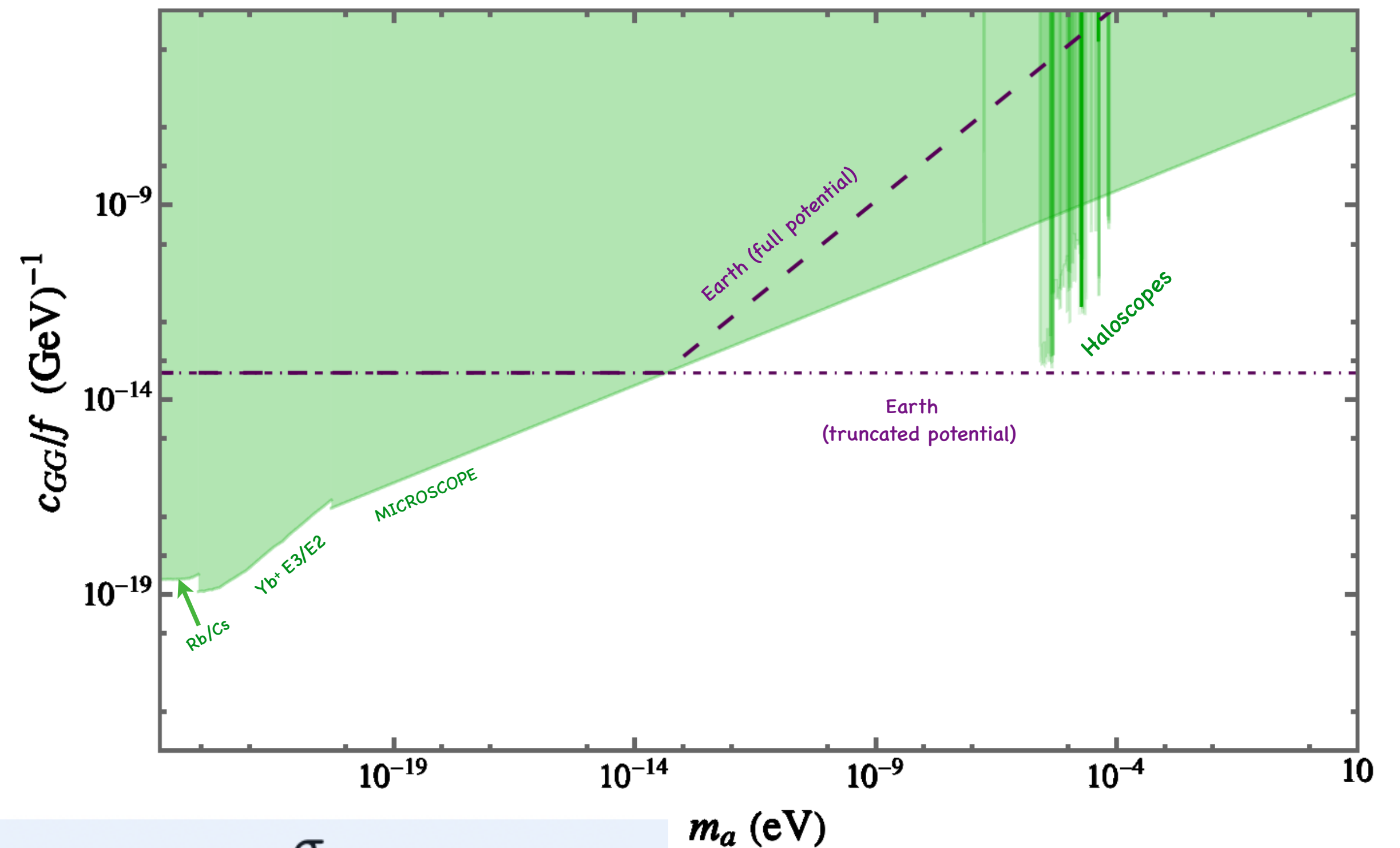
$$\delta_e = \frac{\alpha}{16\pi^2} \ln \frac{m_e^2}{m_\pi^2} \left( 1 - 32c_1 \frac{m_\pi^2}{M_N} \right) \delta_\pi$$

critical value of the axion-gluon  
coupling under the small-coupling  
approximation

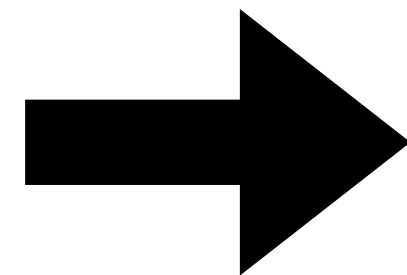


- Axion potential is periodic, resulting in a cutoff for the field value  $a \sim \pi/f$ , implying that the higher order operators in the expansion regulates the divergence in the field.
- For non-DM axion, the boundary condition at  $r \rightarrow \infty$  is a vanishing field value, so the full solution can be obtained. In the case of axion dark matter it should be finite as the free oscillating field - **Needs proper treatment**

$$V = -m_\pi^2 f_\pi^2 \epsilon \sqrt{1 - \frac{4m_u m_d}{(m_u + m_d)^2} \sin^2 \left( \frac{a}{2f_a} \right)}.$$



For the axion field value to deviate from the vacuum solution, the potential energy induced by the source needs to be **sufficiently large** to turn the axion mass tachyonic



$$m_a^2 f^2 + \frac{\sigma}{M_N} \rho_N \delta_\pi < 0,$$

$$m_a^2 f^2 < 5 \times 10^{17} c_{GG}^2 \text{ eV}^4.$$



# Non-dark matter axions

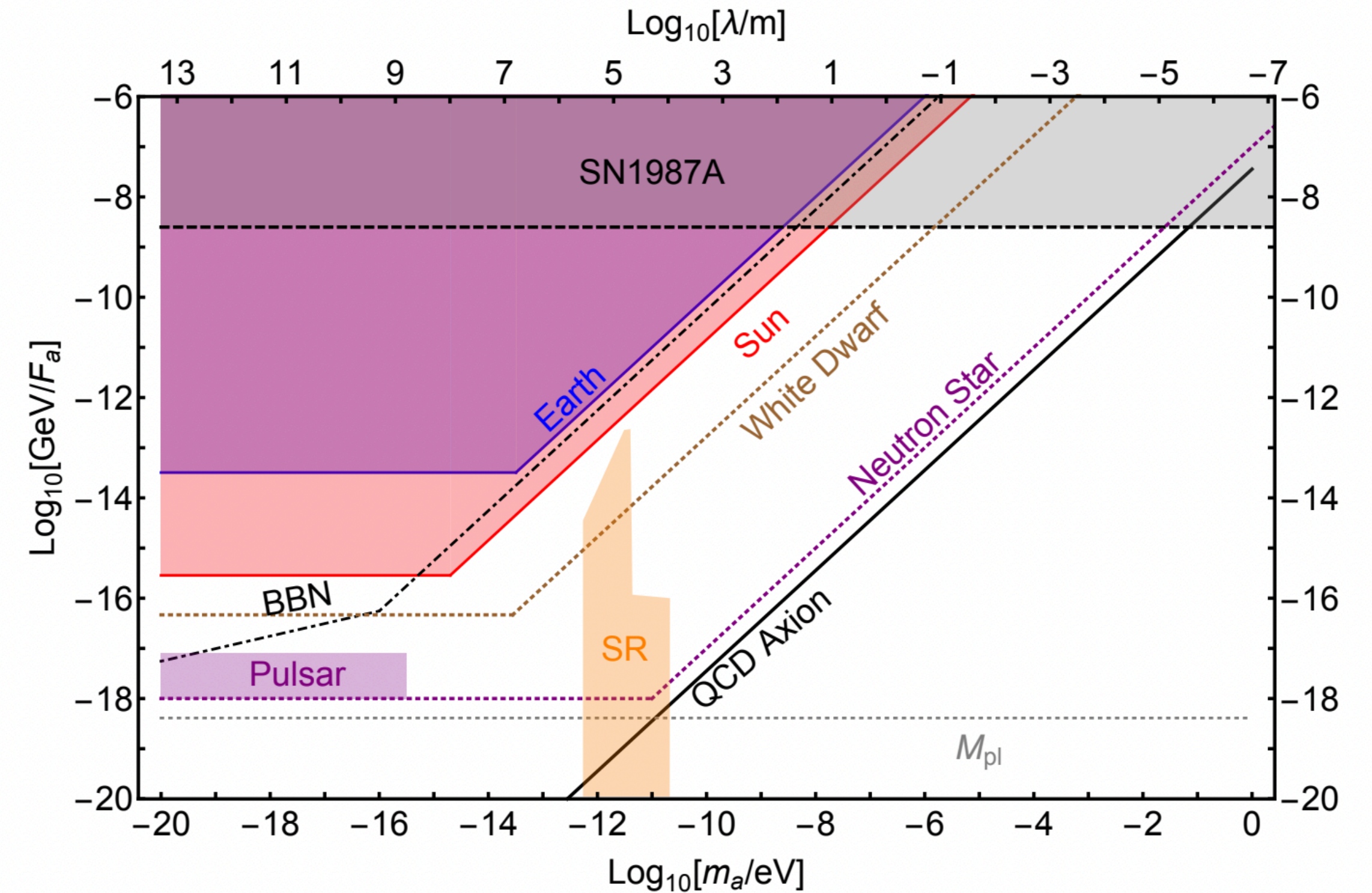
Hook and Huang et. al, 1708.08464

vacuum solution,  $\langle a \rangle = 0$   $m_a \sim m_\pi f_\pi / f_a$

$$V = -m_\pi^2 f_\pi^2 \left\{ \left( \epsilon - \frac{\sigma_N n_N}{m_\pi^2 f_\pi^2} \right) \left| \cos \left( \frac{a}{f_a} \right) \right| + \mathcal{O} \left( \left( \frac{\sigma_N n_N}{m_\pi^2 f_\pi^2} \right)^2 \right) \right\}$$

In a dense  
medium

$$\sigma_N \equiv \sum_{q=u,d} m_q \frac{\partial m_N}{\partial m_q},$$



- gradient energy required to move the axion away from  $a = 0 \sim (f_a^2/r^2)$
- when the energy from the finite density effects overcomes the mass, the minimum of the potential shifts to  $\pi$
- when the gain in potential energy outweighs the gradient energy, the axion gets sourced by the finite density medium

$$r_{\text{crit}} \gtrsim \frac{1}{m_T}, \quad m_T = m_\pi f_\pi \frac{\sqrt{\frac{\sigma_N n_N}{m_\pi^2 f_\pi^2} - \epsilon}}{2f_a}$$